Siegmund Brandt
Hans Dieter Dahmen

The Picture Book of Quantum Mechanics

4th Edition

Siegmund Brandt • Hans Dieter Dahmen

The Picture Book of Quantum Mechanics

Fourth Edition

Springer

Siegmund Brandt
Physics Department
University of Siegen
D-57068 Siegen
Germany
brandt@physik.uni-siegen.de

Hans Dieter Dahmen
Physics Department
University of Siegen
D-57068 Siegen
Germany
dahmen@physik.uni-siegen.de

Please note that additional material for this book can be downloaded from
http://extras.springer.com

ISBN 978-1-4614-3950-9 ISBN 978-1-4614-3951-6 (eBook)
DOI 10.1007/978-1-4614-3951-6
Springer New York Heidelberg Dordrecht London

Library of Congress Control Number: 2012937850

Printed on acid-free paper

Springer is part of Springer Science+Business Media (www.springer.com)

Contents

Preface to the Fourth Edition v
Foreword vii

1 Introduction 1
1.1 The Photoelectric Effect 2
1.2 The Compton Effect 4
1.3 The Diffraction of Electrons 6
1.4 The Stern–Gerlach Experiment 7

2 Light Wavess 11
2.1 Harmonic Plane Waves, Phase Velocity 11
2.2 Light Wave Incident on a Glass Surface 15
2.3 Light Wave Traveling through a Glass Plate 18
2.4 Free Wave Packet 20
2.5 Wave Packet Incident on a Glass Surface 25
2.6 Wave Packet Traveling through a Glass Plate 30

3 Probability Waves of Matter 32
3.1 de Broglie Waves 32
3.2 Wave Packet, Dispersion 32
3.3 Probability Interpretation, Uncertainty Principle 37
3.4 The Schrödinger Equation 46
3.5 Bivariate Gaussian Probability Density 47
3.6 Comparison with a Classical Statistical Description 50

4 Solution of the Schrödinger Equation in One Dimension . . . 56
4.1 Separation of Time and Space Coordinates, Stationary Solutions 56
4.2 Stationary Scattering Solutions: Piecewise Constant Potential 58
4.3 Stationary Scattering Solutions: Linear Potentials 68
4.4 Stationary Bound States 72

5 One-Dimensional Quantum Mechanics: Scattering by a Potential 78
5.1 Sudden Acceleration and Deceleration of a Particle 78
5.2 Sudden Deceleration of a Classical Phase-Space Distribution 83
5.3 Tunnel Effect 85
5.4 Excitation and Decay of Metastable States 86
5.5 Stationary States of Sharp Momentum 91
5.6 Free Fall of a Body 97
5.7 Scattering by a Piecewise Linear Potential 102

6 One-Dimensional Quantum Mechanics: Motion within a Potential, Stationary Bound States 111
6.1 Spectrum of a Deep Square Well 111
6.2 Particle Motion in a Deep Square Well 112
6.3 Spectrum of the Harmonic-Oscillator Potential 116
6.4 Harmonic Particle Motion 119
6.5 Harmonic Motion of a Classical Phase-Space Distribution . 126
6.6 Spectra of Square-Well Potentials of Finite Depths 129
6.7 Stationary Bound States in Piecewise Linear Potentials . . 131
6.8 Periodic Potentials, Band Spectra 133

7 Quantile Motion in One Dimension 141
7.1 Quantile Motion and Tunneling 141
7.2 Probability Current, Continuity Equation 143
7.3 Probability Current Densities of Simple Examples 147
7.4 Differential Equation of the Quantile Trajectory 149
7.5 Error Function 149
7.6 Quantile Trajectories for Simple Examples 150
7.7 Relation to Bohm's Equation of Motion 153

8 Coupled Harmonic Oscillators: Distinguishable Particles . . . 157
8.1 The Two-Particle Wave Function 157
8.2 Coupled Harmonic Oscillators 159
8.3 Stationary States 167

9 Coupled Harmonic Oscillators: Indistinguishable Particles . . 170
9.1 The Two-Particle Wave Function for Indistinguishable Particles 170
9.2 Stationary States 173
9.3 Motion of Wave Packets 174
9.4 Indistinguishable Particles from a Classical Point of View . 175

10 Wave Packet in Three Dimensions 185
10.1 Momentum 185
10.2 Quantile Motion, Probability Transport 187
10.3 Angular Momentum, Spherical Harmonics 191
10.4 Means and Variances of the Components of Angular Momentum 199
10.5 Interpretation of the Eigenfunctions of Angular Momentum 201
10.6 Schrödinger Equation 208
10.7 Solution of the Schrödinger Equation of Free Motion . . . 210
10.8 Spherical Bessel Functions 210
10.9 Harmonic Plane Wave in Angular-Momentum Representation 214
10.10 Free Wave Packet and Partial-Wave Decomposition 218

11 Solution of the Schrödinger Equation in Three Dimensions . . 225
11.1 Stationary Scattering Solutions 226
11.2 Stationary Bound States 229

12 Three-Dimensional Quantum Mechanics: Scattering by a Potential 232
12.1 Diffraction of a Harmonic Plane Wave. Partial Waves . . . 232
12.2 Scattered Wave and Scattering Cross Section 234
12.3 Scattering Phase and Amplitude, Unitarity, Argand Diagrams 244

13 Three-Dimensional Quantum Mechanics: Bound States 251
13.1 Bound States in a Spherical Square-Well Potential 251
13.2 Bound States of the Spherically Symmetric Harmonic Oscillator 257
13.3 Harmonic Particle Motion in Three Dimensions 265
13.4 The Hydrogen Atom 267
13.5 Kepler Motion in Quantum Mechanics 282

14 Hybridization 294
14.1 Introduction 294
14.2 The Hybridization Model 297
14.3 Highly Symmetric Hybrid States 302

15 Three-Dimensional Quantum Mechanics: Resonance Scattering 311
15.1 Scattering by Attractive Potentials 311
15.2 Resonance Scattering 314
15.3 Phase-Shift Analysis 314
15.4 Bound States and Resonances 322
15.5 Resonance Scattering by a Repulsive Shell 325

16 Coulomb Scattering 337
16.1 Stationary Solutions 337
16.2 Hyperbolic Kepler Motion: Scattering of a Gaussian Wave Packet by a Coulomb Potential 346

17 Spin 353
17.1 Spin States, Operators and Eigenvalues 353
17.2 Directional Distribution of Spin 355
17.3 Motion of Magnetic Moments in a Magnetic Field. Pauli Equation 359
17.4 Magnetic Resonance. Rabi's Formula 363
17.5 Magnetic Resonance in a Rotating Frame of Reference . . 369

18 Examples from Experiment 373
18.1 Scattering of Atoms, Electrons, Neutrons, and Pions 374
18.2 Spectra of Bound States in Atoms, Nuclei, and Crystals . . 377
18.3 Shell-Model Classification of Atoms and Nuclei 380
18.4 Resonance Scattering off Molecules, Atoms, Nuclei, and Particles 387
18.5 Phase-Shift Analysis in Nuclear and Particle Physics 391
18.6 Classification of Resonances on Regge Trajectories 393
18.7 Radioactive Nuclei as Metastable States 395
18.8 Magnetic-Resonance Experiments 396

A Simple Aspects of the Structure of Quantum Mechanics 413
A.1 Wave Mechanics 413
A.2 Matrix Mechanics in an Infinite Vector Space 415
A.3 Matrix Representation of the Harmonic Oscillator 419
A.4 Time-Dependent Schrödinger Equation 421
A.5 Probability Interpretation 423

B Two-Level System 425

C Analyzing Amplitude 430
C.1 Classical Considerations: Phase-Space Analysis 430
C.2 Analyzing Amplitude: Free Particle 434
C.3 Analyzing Amplitude: General Case 439
C.4 Analyzing Amplitude: Harmonic Oscillator 439

D Wigner Distribution 446

E Gamma Function 450

F Bessel Functions and Airy Functions 455

G Poisson Distribution 460

Index 465

1. Introduction

The basic fields of classical physics are mechanics and heat on the one hand and electromagnetism and optics on the other. Mechanical and heat phenomena involve the motion of particles as governed by Newton's equations. Electromagnetism and optics deal with fields and waves, which are described by Maxwell's equations. In the classical description of particle motion, the position of the particle is exactly determined at any given moment. Wave phenomena, in contrast, are characterized by interference patterns which extend over a certain region in space. The strict separation of particle and wave physics loses its meaning in atomic and subatomic processes.

Quantum mechanics goes back to Max Planck's discovery in 1900 that the energy of an oscillator of *frequency* ν is quantized. That is, the energy emitted or absorbed by an oscillator can take only the values $0, h\nu, 2h\nu, \ldots$. Only multiples of *Planck's quantum of energy*

$$E = h\nu$$

are possible. *Planck's constant*

$$h = 6.262 \times 10^{-34}\ \mathrm{J\,s}$$

is a fundamental constant of nature, the central one of quantum physics. Often it is preferable to use the *angular frequency* $\omega = 2\pi\nu$ of the oscillator and to write Planck's quantum of energy in the form

$$E = \hbar\omega \quad .$$

Here

$$\hbar = \frac{h}{2\pi}$$

is simply Planck's constant divided by 2π. Planck's constant is a very small quantity. Therefore the quantization is not apparent in macroscopic systems. But in atomic and subatomic physics Planck's constant is of fundamental importance. In order to make this statement more precise, we shall look at experiments showing the following fundamental phenomena:

S. Brandt and H.D. Dahmen, *The Picture Book of Quantum Mechanics*,
DOI 10.1007/978-1-4614-3951-6_1, © Springer Science+Business Media New York 2012

- the photoelectric effect,
- the Compton effect,
- the diffraction of electrons,
- the orientation of the magnetic moment of electrons in a magnetic field.

1.1 The Photoelectric Effect

The photoelectric effect was discovered by Heinrich Hertz in 1887. It was studied in more detail by Wilhelm Hallwachs in 1888 and Philipp Lenard in 1902. We discuss here the quantitative experiment, which was first carried out in 1916 by R. A. Millikan. His apparatus is shown schematically in Figure 1.1a. Monochromatic light of variable frequency falls onto a photocathode in a vacuum tube. Opposite the photocathode there is an anode – we assume cathode and anode to consist of the same metal – which is at a negative voltage U with respect to the cathode. Thus the electric field exerts a repelling force on the electrons of charge $-e$ that leave the cathode. Here $e = 1.609 \times 10^{-19}$ Coulomb is the elementary charge. If the electrons reach the anode, they flow back to the cathode through the external circuit, yielding a measurable current I. The kinetic energy of the electrons can therefore be determined by varying the voltage between anode and cathode. The experiment yields the following findings.

1. The electron current sets in, independent of the voltage U, at a frequency ν_0 that is characteristic for the material of the cathode. There is a current only for $\nu > \nu_0$.

2. The voltage U_s at which the current stops flowing depends linearly on the frequency of the light (Figure 1.1b). The kinetic energy E_{kin} of the electrons leaving the cathode then is equal to the potential energy of the electric field between cathode and anode,

$$E_{kin} = eU_s \quad .$$

If we call h/e the proportionality factor between the frequency of the light and the voltage,

$$U_s = \frac{h}{e}(\nu - \nu_0) \quad ,$$

we find that light of frequency ν transfers the kinetic energy eU_s to the electrons kicked out of the material of the cathode. When light has a frequency less than ν_0, no electrons leave the material. If we call

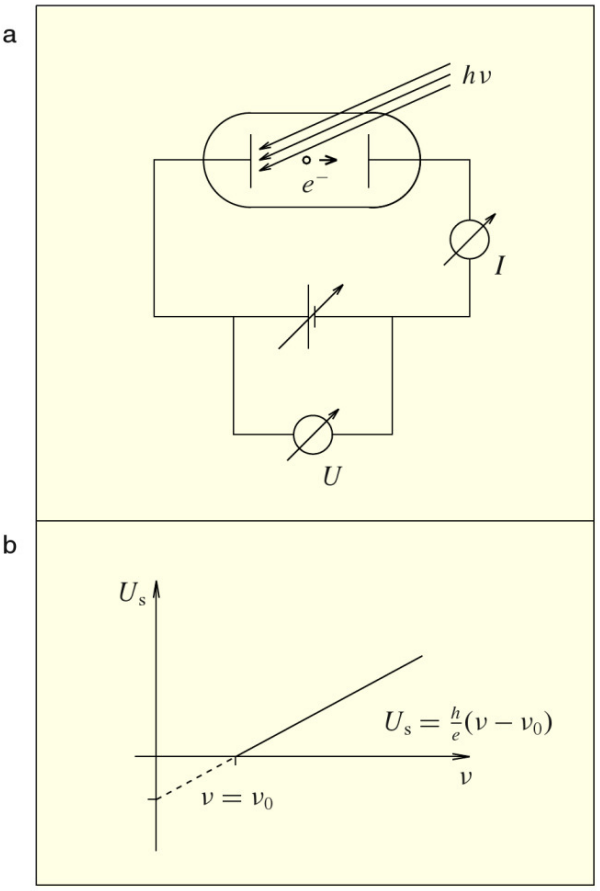

Fig. 1.1. Photoelectric effect. (a) The apparatus to measure the effect consists of a vacuum tube containing two electrodes. Monochromatic light of frequency ν shines on the cathode and liberates electrons which may reach the anode and create a current I in the external circuit. The flow of electrons in the vacuum tube is hindered by the external voltage U. It stops once the voltage exceeds the value U_s. (b) There is a linear dependence between the frequency ν and the voltage U_s.

$$h\nu_0 = eU_k$$

the ionization energy of the material that is needed to free the electrons, we must conclude that light of frequency ν has energy

$$E = h\nu = \hbar\omega$$

with

$$\omega = 2\pi\nu \quad , \qquad \hbar = \frac{h}{2\pi} \quad .$$

3. The number of electrons set free is proportional to the intensity of the light incident on the photocathode.

In 1905 Albert Einstein explained the photoelectric effect by assuming that light consists of quanta of energy $h\nu$ which act in single elementary processes. The *light quanta* are also called *photons* or γ quanta. The number of quanta in the light wave is proportional to its intensity.

1.2 The Compton Effect

If the light quanta of energy $E = h\nu = \hbar\omega$ are particles, they should also have momentum. The relativistic relation between the energy E and momentum p of a particle of rest mass m is

$$p = \frac{1}{c}\sqrt{E^2 - m^2c^4} \quad ,$$

where c is the speed of light in vacuum. Quanta moving with the speed of light must have rest mass zero, so that we have

$$p = \frac{1}{c}\sqrt{\hbar^2\omega^2} = \hbar\frac{\omega}{c} = \hbar k \quad ,$$

where $k = \omega/c$ is the wave number of the light. If the direction of the light is $\mathbf{k}/k$, we find the vectorial relation $\mathbf{p} = \hbar\mathbf{k}$. To check this idea one has to perform an experiment in which light is scattered on free electrons. The conservation of energy and momentum in the scattering process requires that the following relations be fulfilled:

$$\begin{aligned} E_\gamma + E_\mathrm{e} &= E'_\gamma + E'_\mathrm{e} \quad , \\ \mathbf{p}_\gamma + \mathbf{p}_\mathrm{e} &= \mathbf{p}'_\gamma + \mathbf{p}'_\mathrm{e} \quad , \end{aligned}$$

where E_γ, $\mathbf{p}_\gamma$ and E'_γ, $\mathbf{p}'_\gamma$ are the energies and the momenta of the incident and the scattered photon, respectively. E_e, $\mathbf{p}_\mathrm{e}$, E'_e, and $\mathbf{p}'_\mathrm{e}$ are the corresponding quantities of the electron. The relation between electron energy E_e and momentum $\mathbf{p}_\mathrm{e}$ is

$$E_\mathrm{e} = c\sqrt{\mathbf{p}_\mathrm{e}^2 + m_\mathrm{e}^2c^2} \quad ,$$

where m_e is the rest mass of the electron. If the electron is initially at rest, we have $\mathbf{p}_\mathrm{e} = \mathbf{0}$, $E_\mathrm{e} = m_\mathrm{e}c^2$. Altogether, making use of these relations, we obtain

$$\begin{aligned} c\hbar k + m_\mathrm{e}c^2 &= c\hbar k' + c\sqrt{\mathbf{p}_\mathrm{e}'^2 + m_\mathrm{e}^2c^2} \quad , \\ \hbar\mathbf{k} &= \hbar\mathbf{k}' + \mathbf{p}'_\mathrm{e} \end{aligned}$$

as the set of equations determining the wavelength $\lambda' = 2\pi/k'$ of the scattered photon as a function of the wavelength $\lambda = 2\pi/k$ of the initial photon and the scattering angle ϑ (Figure 1.2a). Solving for the difference $\lambda' - \lambda$ of the two wavelengths, we find

$$\lambda' - \lambda = \frac{h}{m_\mathrm{e}c}(1 - \cos\vartheta) \quad .$$

This means that the angular frequency $\omega' = ck' = 2\pi c/\lambda'$ of the light scattered at an angle $\vartheta > 0$ is smaller than the angular frequency $\omega = ck = 2\pi c/\lambda$ of the incident light.

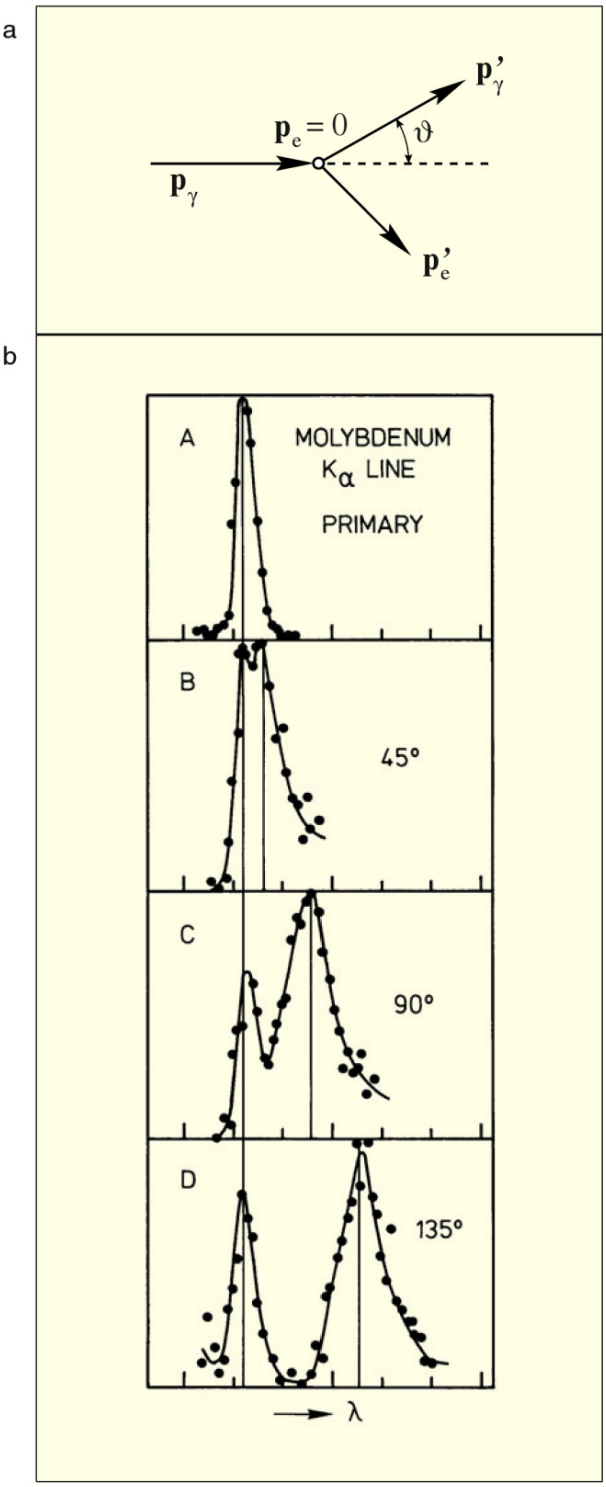

Fig. 1.2. The Compton effect. (a) Kinematics of the process. A photon of momentum $\mathbf{p}_\gamma$ is scattered by a free electron at rest, one with momentum $\mathbf{p}_e = 0$. After the scattering process the two particles have the momenta $\mathbf{p}'_\gamma$ and $\mathbf{p}'_e$, respectively. The direction of the scattered photon forms an angle ϑ with its original direction. From energy and momentum conservation in the collision, the absolute value p'_γ of the momentum of the scattered photon and the corresponding wavelength $\lambda' = h/p'_\gamma$ can be computed. (b) Compton's results. Compton used monochromatic X-rays from the K_α line of molybdenum to bombard a graphite target. The wavelength spectrum of the incident photons shows the rather sharp K_α line at the top. Observations of the photons scattered at three different angles ϑ (45°, 90°, 135°) yielded spectra showing that most of them had drifted to the longer wavelength λ'. There are also many photons at the original wavelength λ, photons which were not scattered by single electrons in the graphite. From A. H. Compton, *The Physical Review* **22** (1923) 409, copyright © 1923 by the American Physical Society, reprinted by permission.

Arthur Compton carried out an experiment in which light was scattered on electrons; he reported in 1923 that the scattered light had shifted to lower frequencies ω' (Figure 1.2b).

1.3 The Diffraction of Electrons

The photoelectric effect and the Compton scattering experiment prove that light must be considered to consist of particles which have rest mass zero, move at the speed of light, and have energy $E = \hbar\omega$ and momentum $\mathbf{p} = \hbar\mathbf{k}$. They behave according to the relativistic laws of particle collisions. The propagation of photons is governed by the wave equation following from Maxwell's equations. The intensity of the light wave at a given location is a measure of the photon density at this point.

Once we have arrived at this conclusion, we wonder whether classical particles such as electrons behave in the same way. In particular, we might conjecture that the motion of electrons should be determined by waves. If the relation $E = \hbar\omega$ between energy and angular frequency also holds for the kinetic energy $E_{\text{kin}} = \mathbf{p}^2/2m$ of a particle moving at nonrelativistic velocity, that is, at a speed small compared to that of light, its angular frequency is given by

$$\omega = \frac{1}{\hbar}\frac{p^2}{2m} = \frac{\hbar k^2}{2m}$$

provided that its wave number k and wavelength λ are related to the momentum p by

$$k = \frac{p}{\hbar} \quad , \qquad \lambda = \frac{h}{p} \quad .$$

Thus the motion of a particle of momentum p is then characterized by a wave with the *de Broglie wavelength* $\lambda = h/p$ and an angular frequency $\omega = p^2/(2m\hbar)$. The concept of matter waves was put forward in 1923 by Louis de Broglie.

If the motion of a particle is indeed characterized by waves, the propagation of electrons should show interference patterns when an electron beam suffers diffraction. This was first demonstrated by Clinton Davisson and Lester Germer in 1927. They observed interference patterns in an experiment in which a crystal was exposed to an electron beam. In their experiment the regular lattice of atoms in a crystal acts like an optical grating. Even simpler conceptually is diffraction from a sharp edge. Such an experiment was performed by Hans Boersch in 1943. He mounted a platinum foil with a sharp edge in the beam of an electron microscope and used the magnification of the microscope to enlarge the interference pattern. Figure 1.3b shows his result. For comparison it is juxtaposed to Figure 1.3a indicating the pattern

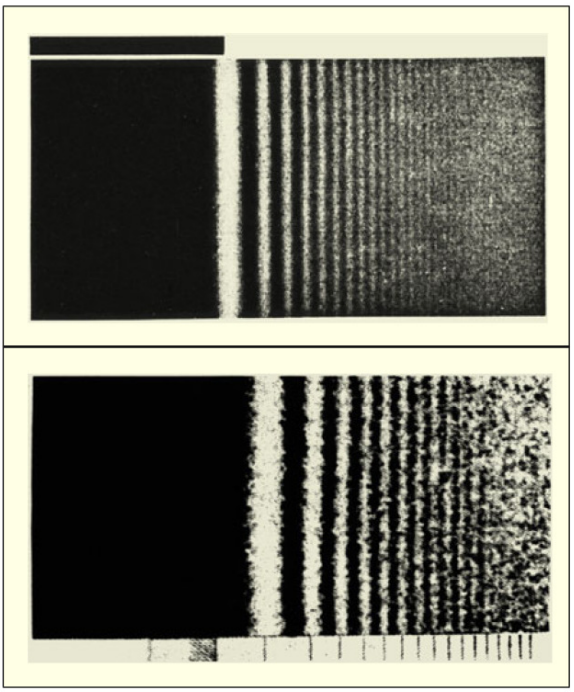

Fig. 1.3. (a) Interference pattern caused by the scattering of red light on a sharp edge. The edge is the border line of an absorbing half-plane, the position of which is indicated at the top of the figure. (b) Interference pattern caused by the scattering of electrons on a sharp edge. *Sources*: (a) From R. W. Pohl, *Optik und Atomphysik*, ninth edition, copyright © 1954 by Springer-Verlag, Berlin, Göttingen, Heidelberg, reprinted by permission. (b) From H. Boersch, *Physikalische Zeitschrift*, **44** (1943) 202, copyright © 1943 by S.-Hirzel-Verlag, Leipzig, reprinted by permission.

produced by visible light diffracted from a sharp edge. The wavelength determined in electron diffraction experiments is in agreement with the formula of de Broglie.

1.4 The Stern–Gerlach Experiment

In 1922 Otto Stern and Walther Gerlach published the result of an experiment in which they measured the magnetic moment of silver atoms. By evaporating silver in an oven with a small aperture they produced a beam of silver atoms which was subjected to a magnetic induction field $\mathbf{B}$. In the coordinate system shown in Figure 1.4 together with the principal components of the experiment the beam travels along the x axis. In the x,z plane the field $\mathbf{B} = (B_x, B_y, B_z)$ has only a z component B_z. Caused by the form of the pole shoes the field is inhomogeneous. The magnitude of B_z is larger near the upper pole shoe which has the shape of a wedge. In the x,z plane the derivative of the field is

$$\frac{\partial \mathbf{B}}{\partial z} = \frac{\partial B_z}{\partial z}\mathbf{e}_z \quad , \qquad \frac{\partial B_z}{\partial z} > 0 \quad .$$

Here $\mathbf{e}_z$ is the unit vector in z direction. In the field a silver atom with the *magnetic moment* $\boldsymbol{\mu}$ experiences the force

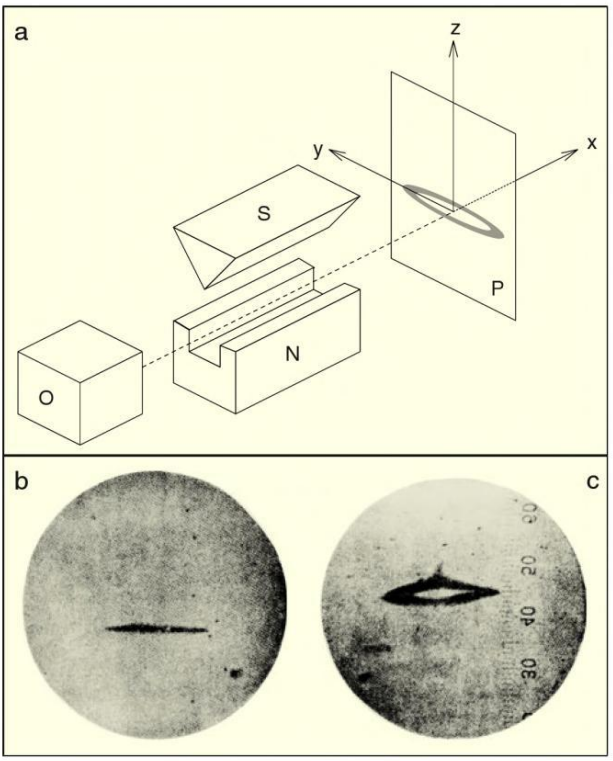

Fig. 1.4. Stern–Gerlach experiment. Experimental setup with oven O, magnet pole shoes N and S, and glass screen P (a). Silver deposit on screen without field (b) and with field (c) as shown in Stern's and Gerlach's original publication. The splitting is largest in the middle and gets smaller to the left and the right of the picture because the field inhomogeneity is largest in the x,z plane. *Source:* (b) and (c) from W. Gerlach and O. Stern, *Zeitschrift für Physik* **9** (1922) 349 © 1922 by Springer-Verlag, Berlin, reprinted by permission.

$$\mathbf{F} = \left(\boldsymbol{\mu} \cdot \frac{\partial \mathbf{B}}{\partial z}\right) \mathbf{e}_z = (\boldsymbol{\mu} \cdot \mathbf{e}_z) \frac{\partial B_z}{\partial z} \mathbf{e}_z \quad .$$

Since the scalar product of $\boldsymbol{\mu}$ and $\mathbf{e}_z$ is

$$\boldsymbol{\mu} \cdot \mathbf{e}_z = \mu \cos \alpha \quad ,$$

where α is the angle between the direction of the magnetic moment and the z direction and μ is the magnitude of the magnetic moment, the force has its maximum strength in the z direction if $\boldsymbol{\mu}$ is parallel to $\mathbf{e}_z$ and its maximum strength in the opposite direction if $\boldsymbol{\mu}$ is antiparallel to $\mathbf{e}_z$. For intermediate orientations the force has intermediate values. In particular, the force vanishes if $\boldsymbol{\mu}$ is perpendicular to $\mathbf{e}_z$, i.e., if $\boldsymbol{\mu}$ is parallel to the x, y plane.

Stern and Gerlach measured the deflection of the silver atoms by this force by placing a glass plate behind the magnet perpendicular to the x axis. In those areas where atoms hit the glass a thin but visible layer of silver formed after some time. Along the z axis they observed two distinct areas of silver indicating that the magnetic moments $\boldsymbol{\mu}$ were oriented preferentially parallel ($\alpha = 0$) or antiparallel ($\alpha = \pi$) to the field $\mathbf{B}$. This finding is contrary to the classical expectation that all orientations of $\boldsymbol{\mu}$ are equally probable.

It remains to be said that the magnetic moment of a silver atom is practically identical to the magnetic moment of a single free electron. A silver atom has 47 electrons but the contributions of 46 electrons to the total magnetic moment cancel. The contribution of the nucleus to the magnetic moment of the atom is very small. The quantitative result of the Stern–Gerlach experiment is

1. The magnetic moment of the electron is

$$\mu = -\frac{e}{m}\frac{\hbar}{2} \quad .$$

2. In the presence of a magnetic field the magnetic moment is found to be oriented parallel or antiparallel to the field direction.

Problems

1.1. Thirty percent of the 100 W power consumption of a sodium lamp goes into the emission of photons with the wavelength $\lambda = 589\,\text{nm}$. How many photons are emitted per second? How many hit the eye of an observer – the diameter of the pupil is 5 mm – stationed 10 km from the lamp?

1.2. The minimum energy $E_0 = h\nu_0$ needed to set electrons free is called the work function of the material. For cesium it is $3.2 \times 10^{-19}\,\text{J}$. What is the minimum frequency and the corresponding maximum wavelength of light that make the photoelectric effect possible? What is the kinetic energy of an electron liberated from a cesium surface by a photon with a wavelength of 400 nm?

1.3. The energy $E = h\nu$ of a light quantum of frequency ν can also be interpreted in terms of Einstein's formula $E = Mc^2$, where c is the velocity of light in a vacuum. (See also the introduction to Chapter 18.) What energy does a blue quantum ($\lambda = 400\,\text{nm}$) lose by moving 10 m upward in the earth's gravitational field? How large is the shift in frequency and wavelength?

1.4. Many radioactive nuclei emit high-energy photons called γ rays. Compute the recoil momentum and velocity of a nucleus possessing 100 times the proton mass and emitting a photon of 1 MeV energy.

1.5. Calculate the maximum change in wavelength experienced by a photon in a Compton collision with an electron initially at rest. The initial wavelength of the photon is $\lambda = 2 \times 10^{-12}\,\text{m}$. What is the kinetic energy of the recoil electron?

1.6. Write the equations for energy and momentum conservation in the Compton scattering process when the electron is not at rest before the collision.

1.7. Use the answer to problem 1.6 to calculate the maximum change of energy and wavelength of a photon of red light ($\lambda = 8 \times 10^{-7}$ m) colliding head on with an electron of energy $E_e = 20$ GeV. (Collisions of photons from a laser with electrons from the Stanford linear accelerator are in fact used to prepare monochromatic high-energy photon beams.)

1.8. Electron microscopes are chosen for very fine resolution because the de Broglie wavelength $\lambda = h/p$ can be made much shorter than the wavelength of visible light. The resolution is roughly λ. Use the relativistic relation $E^2 = p^2c^2 + m^2c^4$ to determine the energy of electrons needed to resolve objects of the size 10^{-6} m (a virus), 10^{-8} m (a DNA molecule), and 10^{-15} m (a proton). Determine the voltage U needed to accelerate the electrons to the necessary kinetic energy $E - mc^2$.

1.9. What are the de Broglie frequency and wavelength of an electron moving with a kinetic energy of 20 keV, which is typical for electrons in the cathode-ray tube of a color television set?

2. Light Wavess

2.1 Harmonic Plane Waves, Phase Velocity

Many important aspects and phenomena of quantum mechanics can be visualized by means of *wave mechanics*, which was set up in close analogy to *wave optics*. Here the simplest building block is the harmonic plane wave of light in a vacuum describing a particularly simple configuration in space and time of the *electric field* **E** and the *magnetic induction field* **B**. If the x axis of a rectangular coordinate system has been oriented parallel to the direction of the wave propagation, the y axis can always be chosen to be parallel to the electric field strength so that the z axis is parallel to the magnetic field strength. With this choice the field strengths can be written as

$$\begin{aligned} E_y &= E_0 \cos(\omega t - kx) \quad , & B_z &= B_0 \cos(\omega t - kx) \quad , \\ E_x &= E_z = 0 \quad , & B_x &= B_y = 0 \quad . \end{aligned}$$

They are shown in Figures 2.1 and 2.2. The quantities E_0 and B_0 are the maximum values reached by the electric and magnetic fields, respectively. They are called *amplitudes*. The *angular frequency* ω is connected to the *wave number* k by the simple relation

$$\omega = ck \quad .$$

The points where the field strength is maximum, that is, has the value E_0, are given by the *phase* of the cosine function

$$\delta = \omega t - kx = 2\ell\pi \quad ,$$

where ℓ takes the integer values $\ell = 0, \pm 1, \pm 2, \ldots$. Therefore such a point moves with the velocity

$$c = \frac{x}{t} = \frac{\omega}{k} \quad .$$

Since this velocity describes the speed of a point with a given phase, c is called the *phase velocity* of the wave. For light waves in a vacuum, it is independent of the wavelength. For positive, or negative, k the propagation is in the direction of the positive, or negative, x axis, respectively.

S. Brandt and H.D. Dahmen, *The Picture Book of Quantum Mechanics*,
DOI 10.1007/978-1-4614-3951-6_2, © Springer Science+Business Media New York 2012

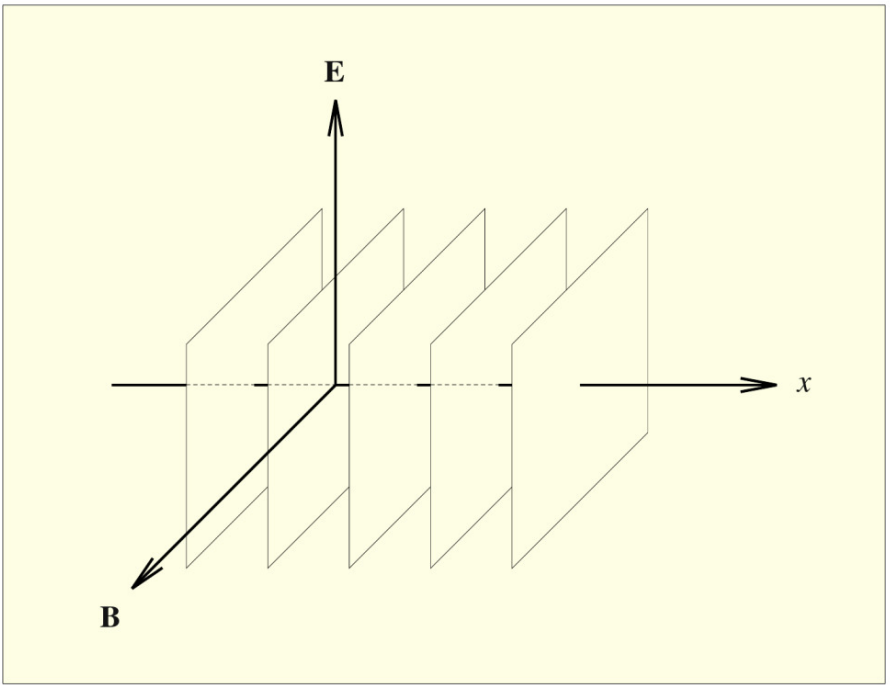

Fig. 2.1. In a plane wave the electric and magnetic field strengths are perpendicular to the direction of propagation. At any moment in time, the fields are constant within planes perpendicular to the direction of motion. As time advances, these planes move with constant velocity.

At a fixed point in space, the field strengths **E** and **B** oscillate in time with the angular frequency ω (Figures 2.3a and c). The *period* of the oscillation is

$$T = \frac{2\pi}{\omega} \quad .$$

For fixed time the field strengths exhibit a periodic pattern in space with a spatial period, the *wavelength*

$$\lambda = \frac{2\pi}{|k|} \quad .$$

The whole pattern moves with velocity c along the x direction. Figures 2.3b and 2.3d present the propagation of waves by a set of curves showing the field strength at a number of consecutive equidistant moments in time. Earlier moments in time are drawn in the background of the picture, later ones toward the foreground. We call such a representation a *time development*.

For our purpose it is sufficient to study only the electric field of a light wave,

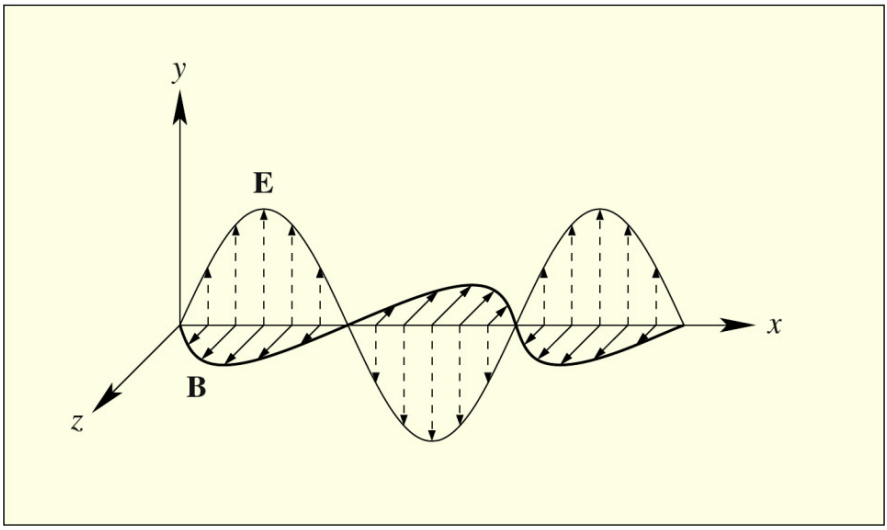

Fig. 2.2. For a given moment in time, the electric field strength E and the magnetic field strength B are shown along a line parallel to the direction of motion of the harmonic plane wave.

$$E_y = E = E_0 \cos(\omega t - kx - \alpha) \quad .$$

We have included an additional *phase* α to allow for the fact that the maximum of E need not be at $x = 0$ for $t = 0$. To simplify many calculations, we now make use of the fact that cosine and sine are equal to the real and imaginary parts of an exponential,

$$\cos\beta + \mathrm{i}\sin\beta = \mathrm{e}^{\mathrm{i}\beta} \quad ,$$

that is,

$$\cos\beta = \mathrm{Re}\,\mathrm{e}^{\mathrm{i}\beta} \quad , \qquad \sin\beta = \mathrm{Im}\,\mathrm{e}^{\mathrm{i}\beta} \quad .$$

The wave is then written as

$$E = \mathrm{Re}\, E_\mathrm{c} \quad ,$$

where E_c is the complex field strength:

$$E_\mathrm{c} = E_0\,\mathrm{e}^{-\mathrm{i}(\omega t - kx - \alpha)} = E_0\,\mathrm{e}^{\mathrm{i}\alpha}\mathrm{e}^{-\mathrm{i}\omega t}\mathrm{e}^{\mathrm{i}kx} \quad .$$

It factors into a complex amplitude

$$A = E_0\,\mathrm{e}^{\mathrm{i}\alpha}$$

and two exponentials containing the time and space dependences, respectively. As mentioned earlier, the wave travels in the positive or negative x

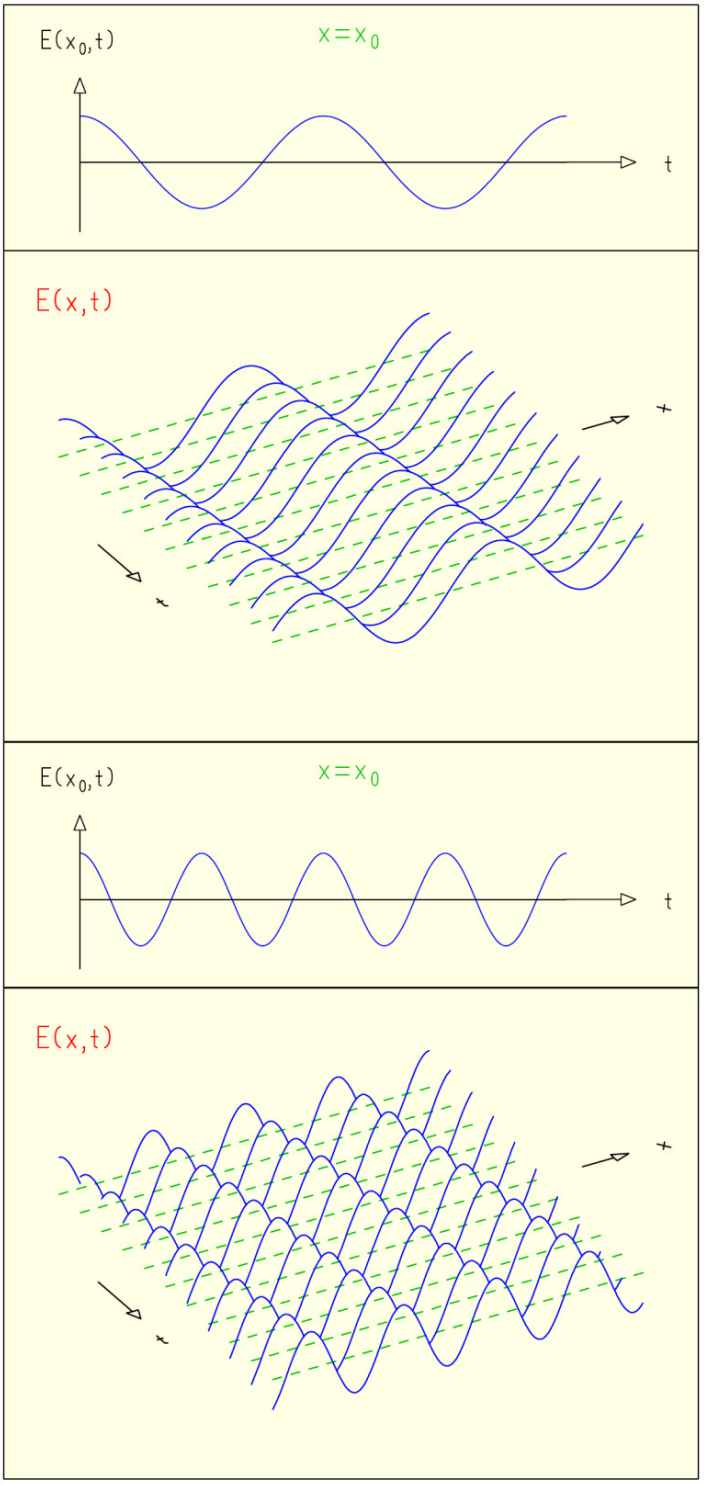

Fig. 2.3. (a) Time dependence of the electric field of a harmonic wave at a fixed point in space. (b) Time development of the electric field of a harmonic wave. The field distribution along the x direction is shown for several moments in time. Early moments are in the background, later moments in the foreground. (c, d) Here the wave has twice the frequency. We observe that the period T and the wavelength λ are halved, but that the phase velocity c stays the same. The time developments in parts b and d are drawn for the same interval of time.

direction, depending on the sign of k. Such waves with different amplitudes are

$$E_{c+} = A\,e^{-i\omega t}e^{ikx} \quad , \qquad E_{c-} = B\,e^{-i\omega t}e^{-ikx} \quad .$$

The factorization into a time- and a space-dependent factor is particularly convenient in solving Maxwell's equations. It allows the separation of time and space coordinates in these equations. If we divide by $\exp(-i\omega t)$, we arrive at the time-independent expressions

$$E_{s+} = A\,e^{ikx} \quad , \qquad E_{s-} = B\,e^{-ikx} \quad ,$$

which we call *stationary waves*.

The *energy density* in an electromagnetic wave is equal to a constant, ε_0, times the square of the field strength,

$$w(x,t) = \varepsilon_0 E^2 \quad .$$

Because the plane wave has a cosine structure, the energy density varies twice as fast as the field strength. It remains always a positive quantity; therefore the variation occurs around a nonzero average value. This average taken over a period T of the wave can be written in terms of the complex field strength as

$$w = \frac{\varepsilon_0}{2} E_c E_c^* = \frac{\varepsilon_0}{2} |E_c|^2 \quad .$$

Here E_c^* stands for the complex conjugate,

$$E_c^* = \mathrm{Re}\,E_c - i\,\mathrm{Im}\,E_c \quad ,$$

of the complex field strength,

$$E_c = \mathrm{Re}\,E_c + i\,\mathrm{Im}\,E_c \quad .$$

For the average energy density in the plane wave, we obtain

$$w = \frac{\varepsilon_0}{2} |A|^2 = \frac{\varepsilon_0}{2} E_0^2 \quad .$$

2.2 Light Wave Incident on a Glass Surface

The effect of glass on light is to reduce the phase velocity by a factor n called the *refractive index*,

$$c' = \frac{c}{n} \quad .$$

Although the frequency ω stays constant, wave number and wavelength are changed according to

$$k' = nk \quad , \qquad \lambda' = \frac{\lambda}{n} \quad .$$

The Maxwell equations, which govern all electromagnetic phenomena, demand the continuity of the electric field strength and its first derivative at the boundaries of the regions with different refractive indices. We consider a wave traveling in the x direction and encountering at position $x = x_1$ the surface of a glass block filling half of space (Figure 2.4a). The surface is oriented perpendicular to the direction of the light. The complex expression

$$E_{1+} = A_1 \mathrm{e}^{\mathrm{i}k_1 x}$$

describes the incident stationary wave to the left of the glass surface, that is, for $x < x_1$, where A_1 is the known amplitude of the incident light wave. At the surface only a part of the light wave enters the glass block; the other part will be reflected. Thus, in the region to the left of the glass block, $x < x_1$, we find in addition to the incident wave the reflected stationary wave

$$E_{1-} = B_1 \mathrm{e}^{-\mathrm{i}k_1 x}$$

propagating in the opposite direction. Within the glass the transmitted wave

$$E_2 = A_2 \mathrm{e}^{\mathrm{i}k_2 x}$$

propagates with the wave number

$$k_2 = n_2 k_1$$

altered by the refractive index $n = n_2$ of the glass. The waves E_{1+}, E_{1-}, and E_2 are called *incoming*, *reflected*, and *transmitted constituent waves*, respectively. The continuity for the field strength E and its derivative E' at $x = x_1$ means that

$$E_1(x_1) = E_{1+}(x_1) + E_{1-}(x_1) = E_2(x_1)$$

and

$$E_1'(x_1) = \mathrm{i}k_1 \left[E_{1+}(x_1) - E_{1-}(x_1)\right] = \mathrm{i}k_2 E_2(x_1) = E_2'(x_1) \quad .$$

The two unknown amplitudes, B_1 of the reflected wave, and A_2 of the transmitted, can now be calculated from these two continuity equations. The electric field in the whole space is determined by two expressions incorporating these amplitudes,

$$E_s = \begin{cases} A_1 \mathrm{e}^{\mathrm{i}k_1 x} + B_1 \mathrm{e}^{-\mathrm{i}k_1 x} & \text{for } x < x_1 \\ A_2 \mathrm{e}^{\mathrm{i}k_2 x} & \text{for } x > x_1 \end{cases} \quad .$$

The electric field in the whole space is obtained as a superposition of constituent waves physically existing in regions 1 and 2. By multiplication with the time-dependent phase $\exp(-\mathrm{i}\omega t)$, we obtain the complex field strength E_c, the real part of which is the physical electric field strength.

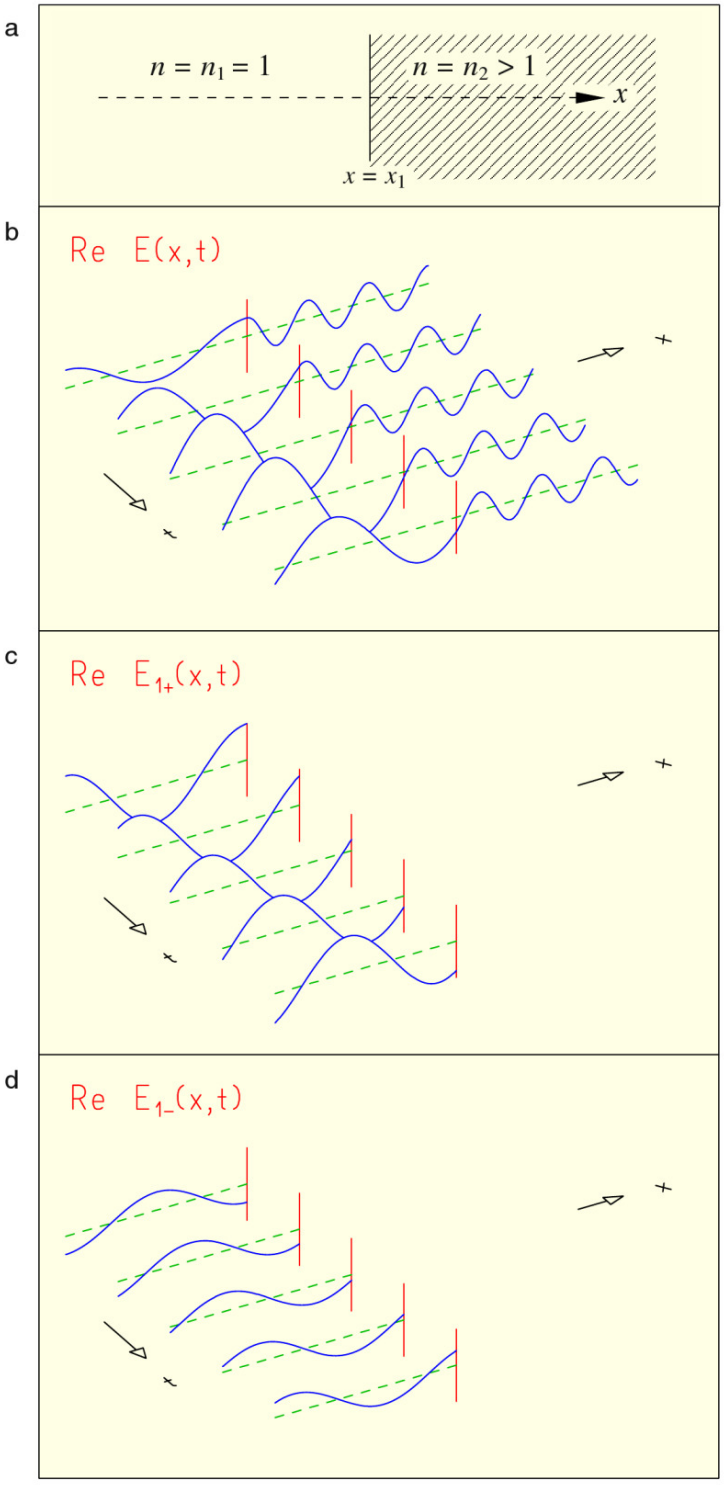

Fig. 2.4. (a) To the right of the plane $x = x_1$, a glass block extends with refractive index $n = n_2$; to the left there is empty space, $n = 1$. (b) Time development of the electric field strength of a harmonic wave which falls from the left onto a glass surface, represented by the vertical line, and is partly reflected by and partly transmitted into the glass. (c) Time development of the incoming wave alone. (d) Time development of the reflected wave alone.

Figure 2.4b gives the time development of this electric field strength. It is easy to see that in the glass there is a harmonic wave moving to the right. The picture in front of the glass is less clear. Figures 2.4c and d therefore show separately the time developments of the incoming and the reflected waves which add up to the total wave to the left of x_1, observed in Figure 2.4b.

2.3 Light Wave Traveling through a Glass Plate

It is now easy to see what happens when light falls on a glass plate of finite thickness. When the light wave penetrates the front surface at $x = x_1$, again reflection occurs so that we have as before the superposition of two stationary waves in the region $x < x_1$:

$$E_1 = A_1 e^{ik_1 x} + B_1 e^{-ik_1 x} \quad .$$

The wave moving within the glass plate suffers reflection at the rear surface at $x = x_2$, so that the second region, $x_1 < x < x_2$, also contains a superposition of two waves,

$$E_2 = A_2 e^{ik_2 x} + B_2 e^{-ik_2 x} \quad ,$$

which now have the refracted wave number

$$k_2 = n_2 k_1 \quad .$$

Only in the third region, $x_2 < x$, do we observe a single stationary wave

$$E_3 = A_3 e^{ik_1 x}$$

with the original wave number k_1.

As a consequence of the reflection on both the front and the rear surface of the glass plate, the reflected wave in region 1 consists of two parts which interfere with each other. The most prominent phenomenon observed under appropriate circumstances is the destructive interference between these two reflected waves, so that no reflection remains in region 1. The light wave is completely transmitted into region 3. This phenomenon is called a *resonance of transmission*. It can be illustrated by looking at the *frequency dependence* of the stationary waves. The upper plot of Figure 2.5 shows the stationary waves for different fixed values of the angular frequency ω, with its magnitude rising from the background to the foreground. A resonance of transmission is recognized through a maximum in the amplitude of the transmitted wave, that is, in the wave to the right of the glass plate.

The signature of a resonance becomes even more prominent in the frequency dependence of the average energy density in the wave. As discussed in Section 2.1, in a vacuum the average energy density has the form

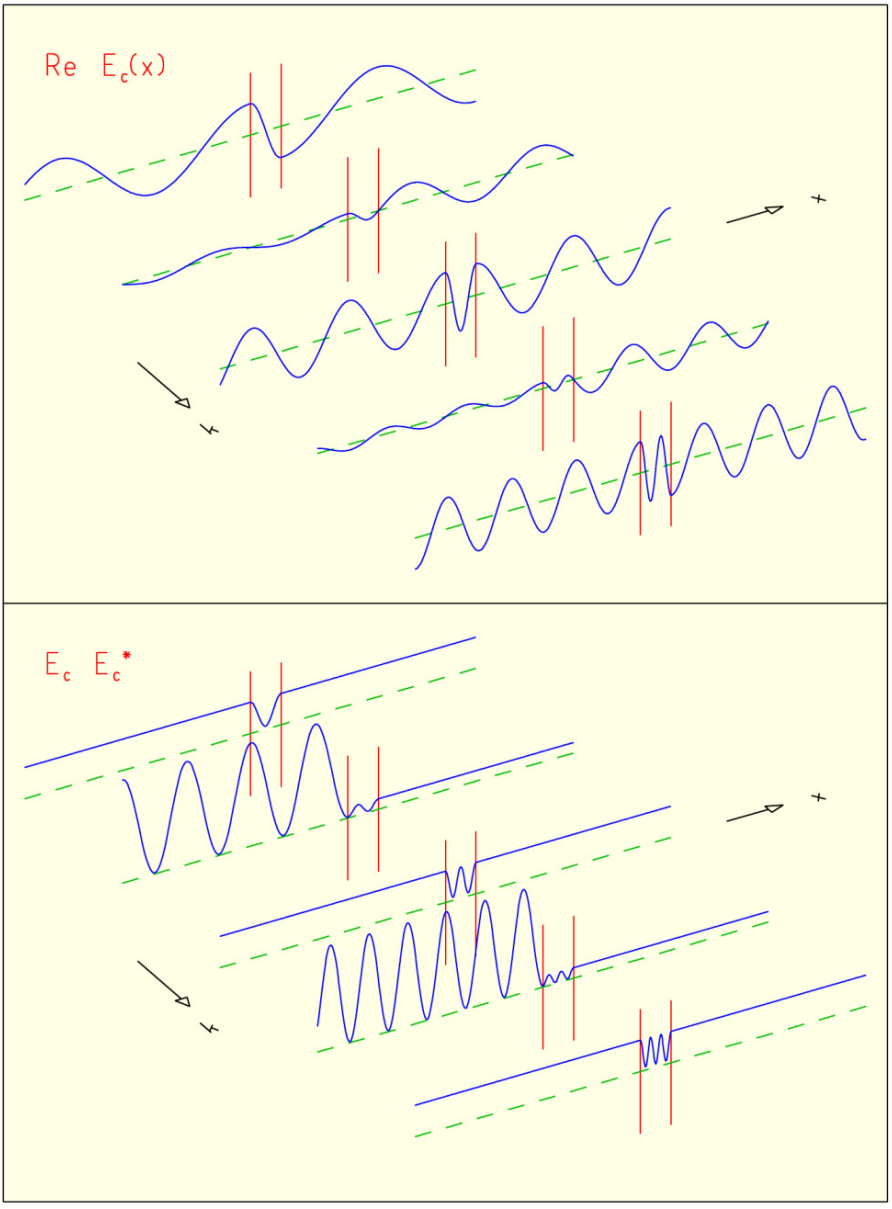

Fig. 2.5. Top: Frequency dependence of stationary waves when a harmonic wave is incident from the left on a glass plate. The two vertical lines indicate the thickness of the plate. Small values of the angular frequency ω are given in the background, large values in the foreground of the picture. Bottom: Frequency dependence of the quantity $E_c E_c^*$ (which except for a factor n_2 is proportional to the average energy density) of a harmonic wave incident from the left on a glass plate. The parameters are the same as in part a. At a resonance of transmission, the average energy density is constant in the left region, indicating through the absence of interference wiggles that there is no reflection.

$$w = \frac{\varepsilon_0}{2} E_c E_c^* \quad .$$

In glass, where the refractive index n has to be taken into account, we have

$$w = \frac{\varepsilon\varepsilon_0}{2} E_c E_c^* = n^2 \frac{\varepsilon_0}{2} E_c E_c^* \quad ,$$

where $\varepsilon = n^2$ is the dielectric constant of glass. Thus, although E_c is continuous at the glass surface, w is not. It reflects the discontinuity of n^2. Therefore we prefer plotting the continuous quantity

$$\frac{2}{n^2\varepsilon_0} w = E_c E_c^* \quad .$$

This plot, shown in the lower plot of Figure 2.5, indicates a resonance of transmission by the maximum in the average energy density of the transmitted wave. Moreover, since there is no reflected wave at the resonance of transmission, the energy density is constant in region 1.

In the glass plate we observe the typical pattern of a resonance.

(i) The amplitude of the average energy density is maximum.

(ii) The energy density vanishes in a number of places called *nodes* because for a resonance a multiple of half a wavelength fits into the glass plate. Therefore different resonances can be distinguished by the number of nodes.

The ratio of the amplitudes of the transmitted and incident waves is called the *transmission coefficient* of the glass plate,

$$T = \frac{A_3}{A_1} \quad .$$

2.4 Free Wave Packet

The plane wave extends into all space, in contrast to any realistic physical situation in which the wave is localized in a finite domain of space. We therefore introduce the concept of a wave packet. It can be understood as a *superposition*, that is, a sum of plane waves of different frequencies and amplitudes. As a first step we concentrate the wave only in the x direction. It still extends through all space in the y and the z direction. For simplicity we start with the sum of two plane waves with equal amplitudes, E_0:

$$E = E_1 + E_2 = E_0 \cos(\omega_1 t - k_1 x) + E_0 \cos(\omega_2 t - k_2 x) \quad .$$

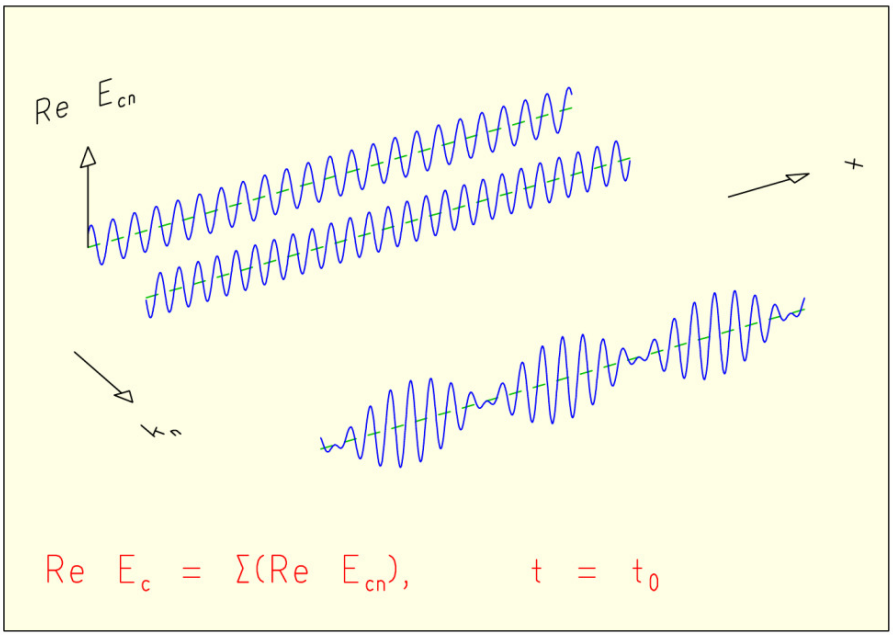

Fig. 2.6. Superposition of two harmonic waves of slightly different angular frequencies ω_1 and ω_2 at a fixed moment in time.

For a fixed time this sum represents a plane wave with two periodic structures. The slowly varying structure is governed by a spatial period,

$$\lambda_- = \frac{4\pi}{|k_2 - k_1|} \quad ,$$

the rapidly varying structure by a wavelength,

$$\lambda_+ = \frac{4\pi}{|k_2 + k_1|} \quad .$$

The resulting wave can be described as the product of a "carrier wave" with the short wavelength λ_+ and a factor modulating its amplitude with the wavelength λ_-:

$$E = 2E_0 \cos(\omega_- t - k_- x)\cos(\omega_+ t - k_+ x) \quad ,$$

$$k_\pm = |k_2 \pm k_1|/2 \quad , \qquad \omega_\pm = c k_\pm \quad .$$

Figure 2.6 plots for a fixed moment in time the two waves E_1 and E_2, and the resulting wave E. Obviously, the field strength is now concentrated for the most part in certain regions of space. These regions of great field strength propagate through space with the velocity

$$\frac{\Delta x}{\Delta t} = \frac{\omega_-}{k_-} = c \quad .$$

Now we again use complex field strengths. The superposition is written as

$$E_c = E_0 \, e^{-i(\omega_1 t - k_1 x)} + E_0 \, e^{-i(\omega_2 t - k_2 x)} \quad .$$

For the sake of simplicity, we have chosen in this example a superposition of two harmonic waves with equal amplitudes. By constructing a more complicated "sum" of plane waves, we can concentrate the field in a single region of space. To this end we superimpose a continuum of waves with different frequencies $\omega = ck$ and amplitudes:

$$E_c(x,t) = E_0 \int_{-\infty}^{+\infty} dk \, f(k) e^{-i(\omega t - kx)} \quad .$$

Such a configuration is called a *wave packet*. The *spectral function* $f(k)$ specifies the amplitude of the harmonic wave with wave number k and circular frequency $\omega = ck$. We now consider a particularly simple spectral function which is significantly different from zero in the neighborhood of the wave number k_0. We choose the *Gaussian* function

$$f(k) = \frac{1}{\sqrt{2\pi}\sigma_k} \exp\left[-\frac{(k-k_0)^2}{2\sigma_k^2} \right] \quad .$$

It describes a bell-shaped spectral function which has its maximum value at $k = k_0$; we assume the value of k_0 to be positive, $k_0 > 0$. The width of the region in which the function $f(k)$ is different from zero is characterized by the parameter σ_k. In short, one speaks of a Gaussian with *width* σ_k. The Gaussian function $f(k)$ is shown in Figure 2.7a. The factors in front of the exponential are chosen so that the area under the curve equals one. We illustrate the construction of a wave packet by replacing the integration over k by a sum over a finite number of terms,

$$\begin{aligned} E_c(x,t) &\approx \sum_{n=-N}^{N} E_n(x,t) \quad , \\ E_n(x,t) &= E_0 \, \Delta k \, f(k_n) e^{-i(\omega_n t - k_n x)} \quad , \end{aligned}$$

where

$$k_n = k_0 + n \, \Delta k \quad , \qquad \omega_n = c k_n \quad .$$

In Figure 2.7b the different terms of this sum are shown for time $t = 0$, together with their sum, which is depicted in the foreground. The term with the lowest wave number, that is, the longest wavelength, is in the background of the picture. The variation in the amplitudes of the different terms reflects

the Gaussian form of the spectral function $f(k)$, which has its maximum, for $k = k_0$, at the center of the picture. On the different terms, the partial waves, the point $x = 0$ is marked by a circle. We observe that the sum over all terms is concentrated around a rather small region near $x = 0$.

Figure 2.7c shows the same wave packet, similarly made up of its partial waves, for later time $t_1 > 0$. The wave packet as well as all partial waves have moved to the right by the distance ct_1. The partial waves still carry marks at the phases that were at $x = 0$ at time $t = 0$. The picture makes it clear that all partial waves have the same velocity as the wave packet, which maintains the same shape for all moments in time.

If we perform the integral explicitly, the wave packet takes the simple form

$$\begin{aligned} E_c(x,t) &= E_c(ct - x) \\ &= E_0 \exp\left[-\frac{\sigma_k^2}{2}(ct - x)^2\right] \exp\left[-i(\omega_0 t - k_0 x)\right] \quad , \end{aligned}$$

that is,

$$E(x,t) = \mathrm{Re}\, E_c = E_0 \exp\left[-\frac{\sigma_k^2}{2}(ct - x)^2\right] \cos(\omega_0 t - k_0 x) \quad .$$

It represents a plane wave propagating in the positive x direction, with a field strength concentrated in a region of the spatial extension $1/\sigma_k$ around point $x = ct$. The time development of the field strength is shown in Figure 2.8b. Obviously, the maximum of the field strength is located at $x = ct$; thus the wave packet moves with the velocity c of light. We call this configuration a *Gaussian wave packet* of spatial width

$$\Delta x = \frac{1}{\sigma_k} \quad ,$$

and of wave-number width

$$\Delta k = \sigma_k \quad .$$

We observe that a spatial concentration of the wave in the region Δx necessarily requires a spectrum of different wave numbers in the interval Δk so that

$$\Delta x\, \Delta k = 1 \quad .$$

This is tantamount to saying that the sharper the localization of the wave packet in x space, the wider is its spectrum in k space. The original harmonic wave $E = E_0 \cos(\omega t - kx)$ was perfectly sharp in k space ($\Delta k = 0$) and therefore not localized in x space. The time development of the average energy density w shown in Figure 2.8c appears even simpler than that of the field

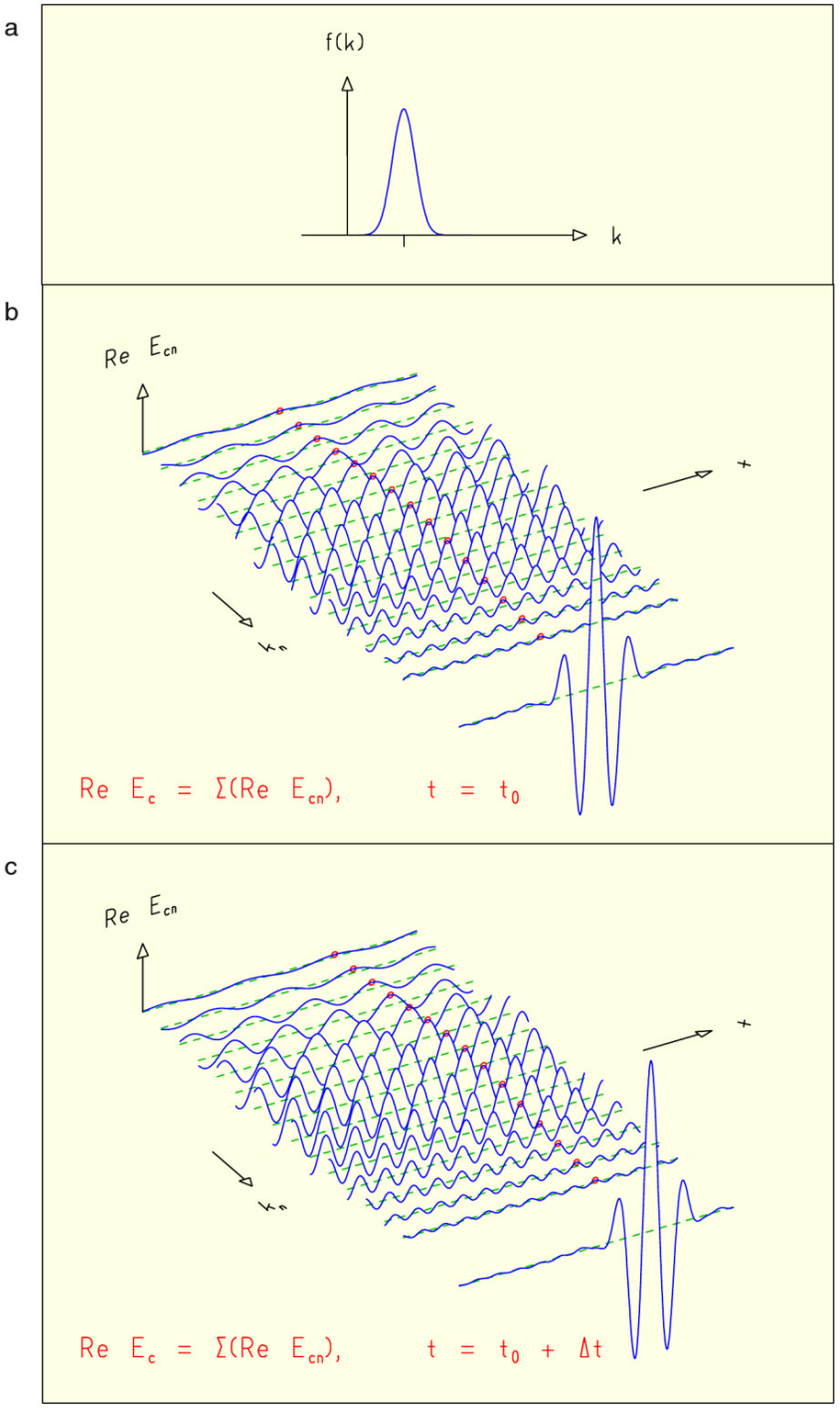

Fig. 2.7.

strength. It is merely a Gaussian traveling with the velocity of light along the x direction. The Gaussian form is easily explained if we remember that

$$w = \frac{\varepsilon_0}{2} E_c E_c^* = \frac{\varepsilon_0}{2} E_0^2 e^{-\sigma_k^2 (ct-x)^2} \quad .$$

We demonstrate the influence of the spectral function on the wave packet by showing in Figure 2.8 spectral functions with two different widths σ_k. For both we show the time development of the field strength and of the average energy density.

2.5 Wave Packet Incident on a Glass Surface

The wave packet, like the plane waves of which it is composed, undergoes reflection and transmission at the glass surface. The upper plot of Figure 2.9 shows the time development of the average energy density in a wave packet moving in from the left. As soon as it hits the glass surface, the already reflected part interferes with the incident wave packet, causing the wiggly structure at the top of the packet. Part of the packet enters the glass, moving with a velocity reduced by the refractive index. For this reason it is compressed in space. The remainder is reflected and moves to the left as a regularly shaped wave packet as soon as it has left the region in front of the glass where interference with the incident packet occurs.

We now demonstrate that the wiggly structure in the interference region is caused by the fast spatial variation of the carrier wave characterized by its wavelength. To this end let us examine the time development of the field strength in the packet, shown in the lower plot of Figure 2.9. Indeed, the spatial variation of the field strength has twice the wavelength of the average energy density in the interference region.

Another way of studying the reflection and transmission of the packet is to look separately at the average energy densities of the constituent waves, namely the incoming, transmitted, and reflected waves. We show these constituent waves in both regions 1, a vacuum, and 2, the glass, although they contribute physically only in either the one or the other. Figure 2.10 gives

Fig. 2.7. (a) Gaussian spectral function describing the amplitudes of harmonic waves of different wave numbers k. (b) Construction of a light wave packet as a sum of harmonic waves of different wavelengths and amplitudes. For time $t = 0$ the different terms of the sum are plotted, starting with the contribution of the longest wavelength in the background. Points $x = 0$ are indicated as circles on the partial waves. The resulting wave packet is shown in the foreground. (c) The same as part b, but for time $t_1 > 0$. The phases that were at $x = 0$ for $t = 0$ have moved to $x_1 = ct_1$ for all partial waves. The wave packet has consequently moved by the same distance and retained its shape.

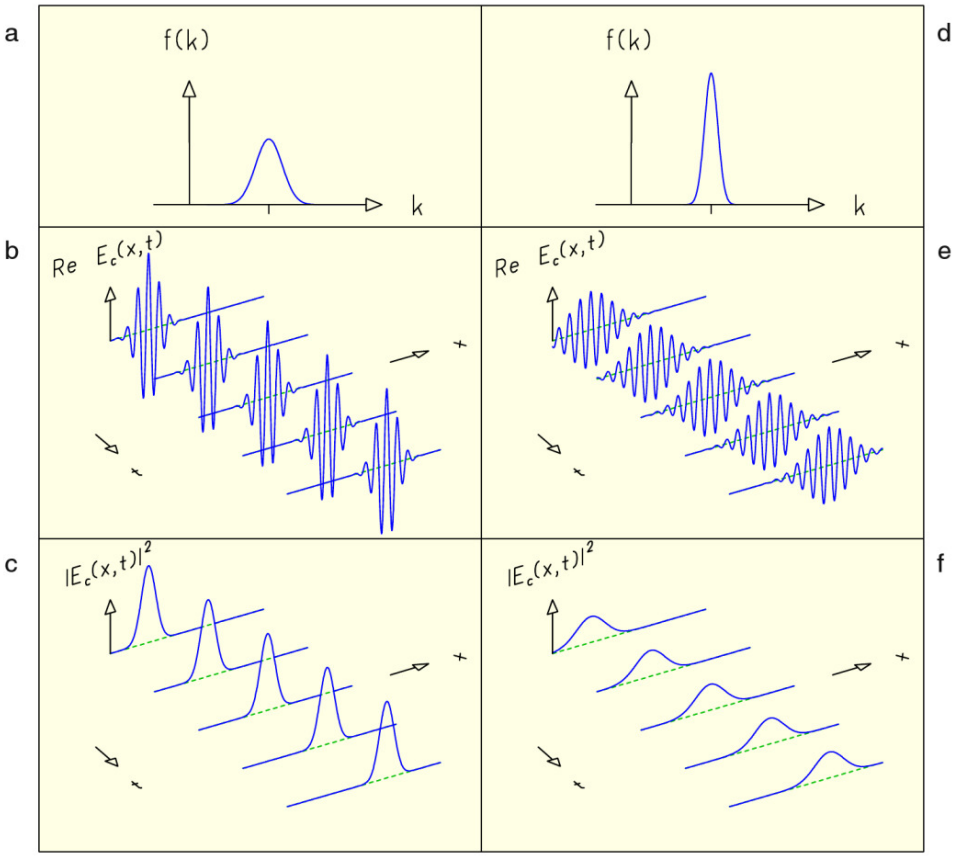

Fig. 2.8. (a, d) Spectral functions, (b, e) time developments of the field strength, and (c, f) time developments of the average energy density for two different Gaussian wave packets.

their time developments. All three have a smooth bell-shaped form and no wiggles, even in the interference region. The time developments of the field strengths of the constituent waves are shown in Figure 2.11. The observed average energy density of Figure 2.9 corresponds to the absolute square of the sum of the incoming and reflected field strengths in the region in front of the glass and, of course, not to the sum of the average energy densities of these two constituent fields. Their interference pattern shows half the wavelength of the carrier waves.

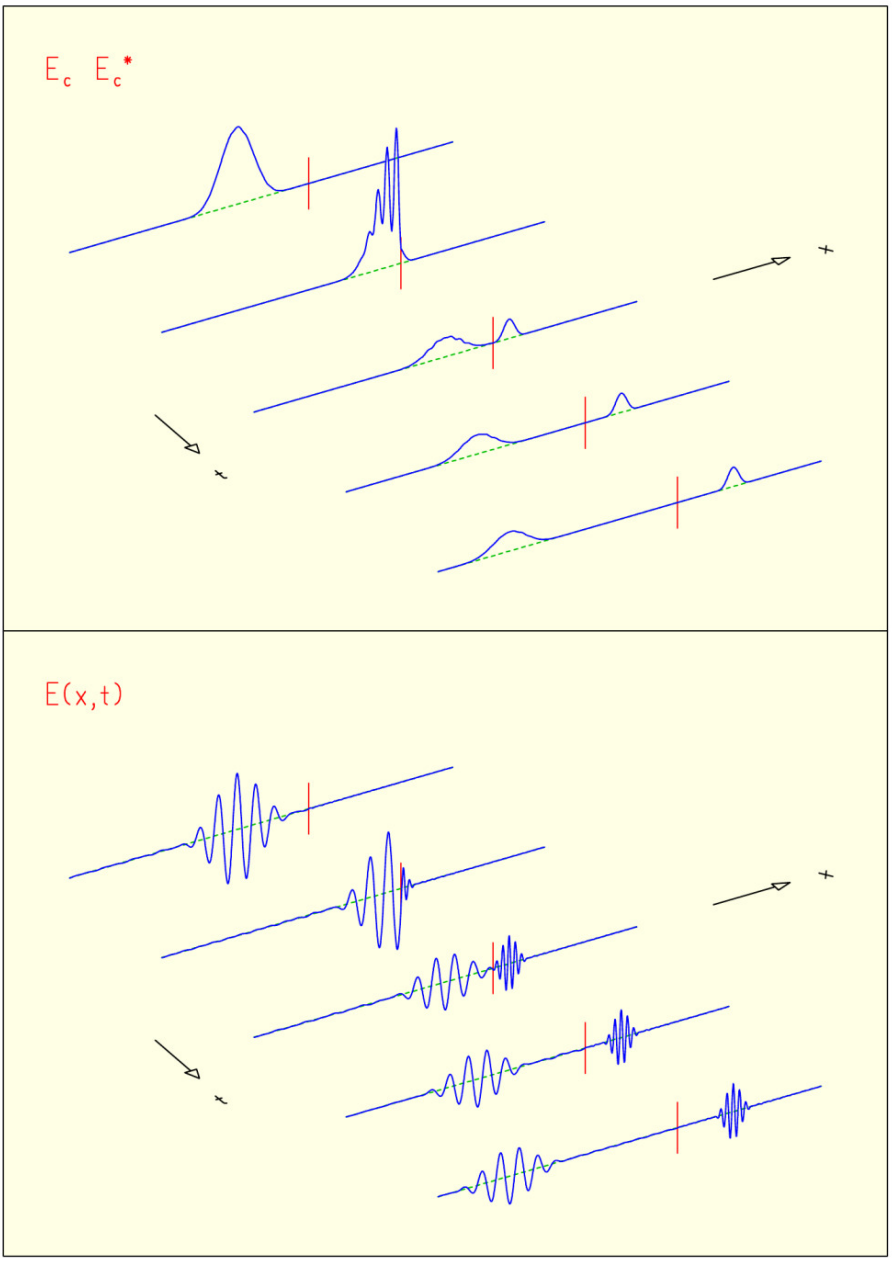

Fig. 2.9. Time developments of the quantity $E_c E_c^*$ (which except for a factor n^2 is proportional to the average energy density) and of the field strength in a wave packet of light falling onto a glass surface where it is partly reflected and partly transmitted through the surface. The glass surface is indicated by the vertical line.

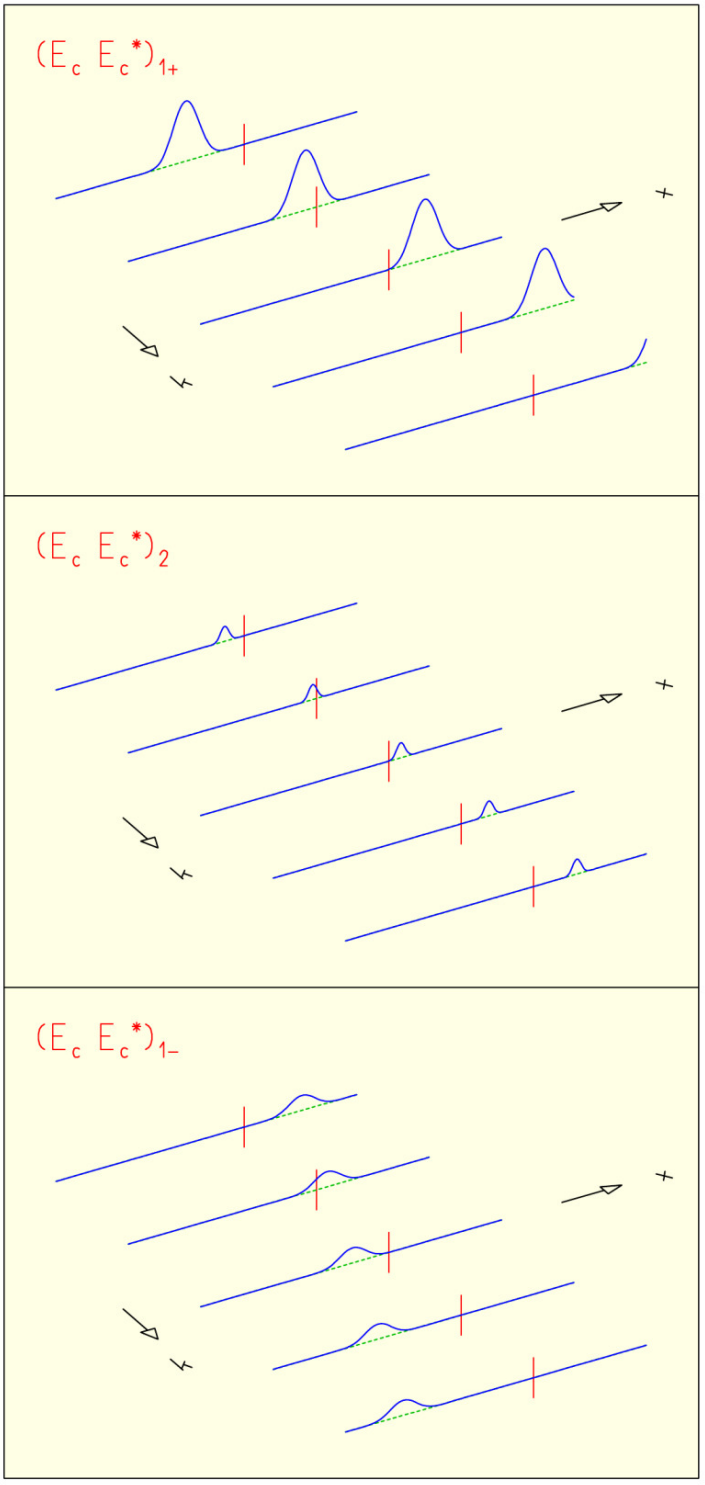

Fig. 2.10. Time developments of the quantity $E_c E_c^*$ (which except for a factor n^2 is proportional to the average energy density) of the constituent waves in a wave packet of light incident on a glass surface: (a) incoming wave, (b) transmitted wave, and (c) reflected wave.

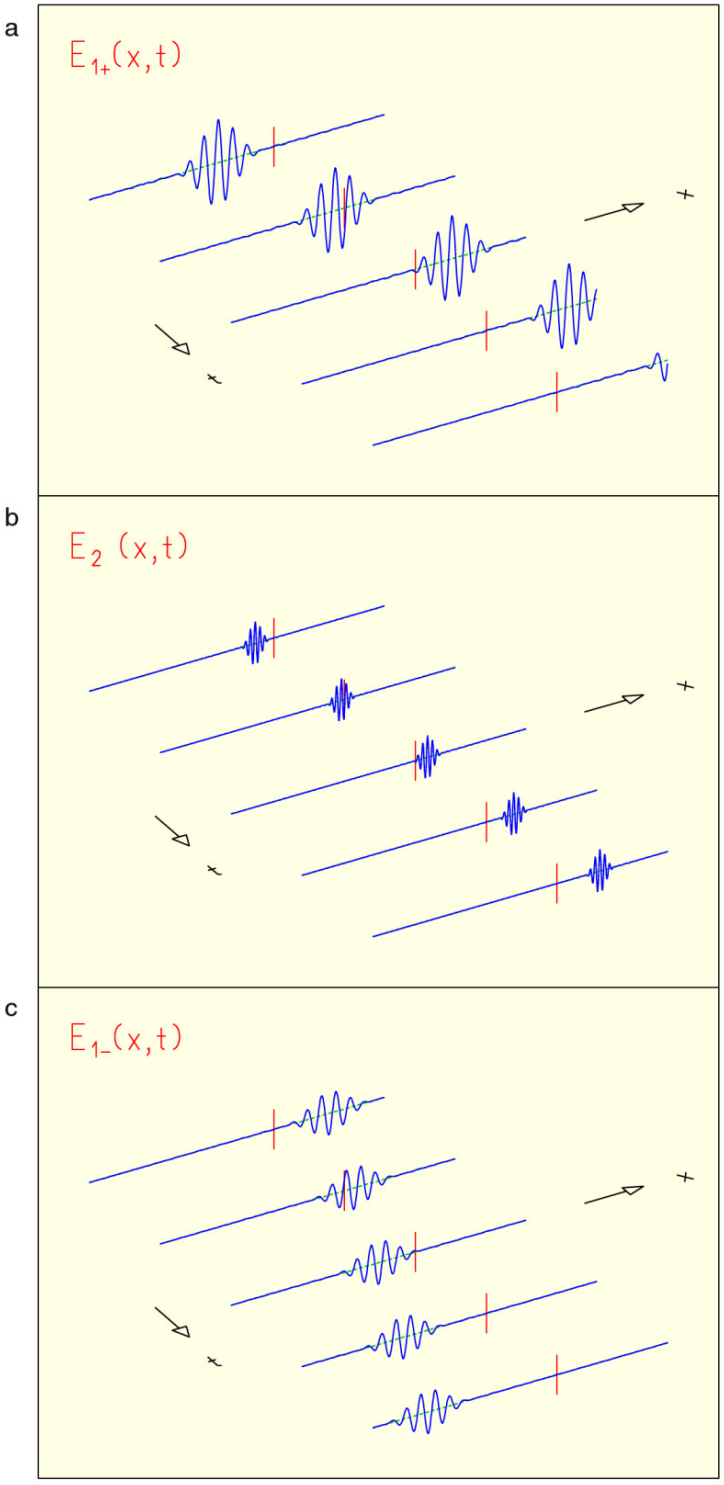

Fig. 2.11. Time developments of the electric field strengths of the constituent waves in a wave packet of light incident on a glass surface: (a) incoming wave, (b) transmitted wave, and (c) reflected wave.

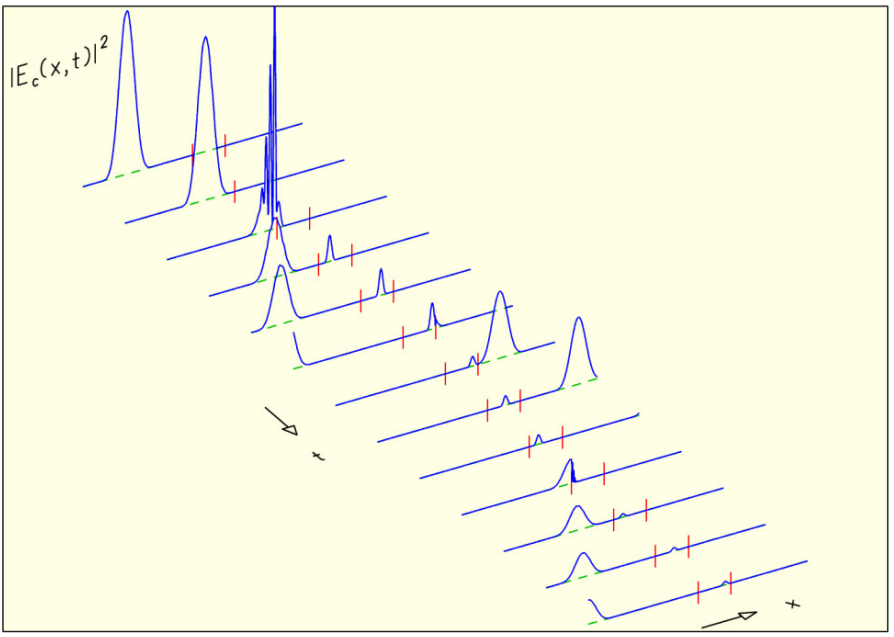

Fig. 2.12. Time development of the quantity $E_c E_c^*$ (which except for a factor n^2 is proportional to the average energy density) in a wave packet of light incident on a glass plate.

2.6 Wave Packet Traveling through a Glass Plate

Let us study a wave packet that is relatively narrow in space, that is, one containing a wide range of frequencies. The time development of its average energy density (Figure 2.12) shows that, as expected, at the front surface of the glass plate part of the packet is reflected. Another part enters the plate, where it is compressed and travels with reduced speed. At the rear surface this packet is again partly reflected while another part leaves the plate, traveling to the right with the original width and speed. The small packet traveling back and forth in the glass suffers multiple reflections on the glass surfaces, each time losing part of its energy to packets leaving the glass.

Problems

2.1. Estimate the refractive index n_2 of the glass plate in Figure 2.4b.

2.2. Calculate the energy density for the plane electromagnetic wave described by the complex electric field strength

localize a particle in space, we again have to superimpose harmonic waves to form a wave packet. To keep things simple, we first restrict ourselves to discussing a one-dimensional wave packet.

For the spectral function we again choose a Gaussian function,[1]

$$f(p) = \frac{1}{(2\pi)^{1/4}\sqrt{\sigma_p}} \exp\left[-\frac{(p-p_0)^2}{4\sigma_p^2}\right] \quad .$$

The corresponding de Broglie wave packet is then

$$\psi(x,t) = \int_{-\infty}^{+\infty} f(p)\psi_p(x-x_0,t)\,\mathrm{d}p \quad .$$

For the de Broglie wave packet, as for the light wave packet, we first approximate the integral by a sum,

$$\psi(x,t) \approx \sum_{n=-N}^{N} \psi_n(x,t) \quad ,$$

where the $\psi_n(x,t)$ are harmonic waves for different values $p_n = p_0 + n\,\Delta p$ multiplied by the spectral weight $f(p_n)\,\Delta p$,

$$\psi_n(x,t) = f(p_n)\psi(x-x_0,t)\,\Delta p \quad .$$

Figure 3.1a shows the real parts $\mathrm{Re}\,\psi_n(x,t)$ of the harmonic waves $\psi_n(x,t)$ as well as their sum being equal to the real part $\mathrm{Re}\,\psi(x,t)$ of the wave function $\psi(x,t)$ for the wave packet at time $t = t_0 = 0$. The point $x = x_0$ is marked on each harmonic wave. In Figure 3.1b the real parts $\mathrm{Re}\,\psi_n(x,t)$ and their sum $\mathrm{Re}\,\psi(x,t)$ are shown at later time $t = t_1$. Because of their different phase velocities, the partial waves have moved by different distances $\Delta x_n = v_n(t_1 - t_0)$ where $v_n = p_n/(2m)$ is the phase velocity of the harmonic wave of momentum p_n. This effect broadens the extension of the wave packet.

The integration over p can be carried out so that the explicit expression for the wave packet has the form

$$\psi(x,t) = M(x,t)\mathrm{e}^{\mathrm{i}\phi(x,t)} \quad .$$

Here the exponential function represents the carrier wave with a *phase* ϕ varying rapidly in space and time. The bell-shaped amplitude function

[1] We have chosen this spectral function to correspond to the square root of the spectral function that was used in Section 2.4 to construct a wave packet of light. Since the area under the spectral function $f(k)$ of Section 2.4 was equal to one, the area under $\left[f(p)\right]^2$ is now equal to one. This guarantees that the normalization condition of the wave function ψ in the next section will be fulfilled.

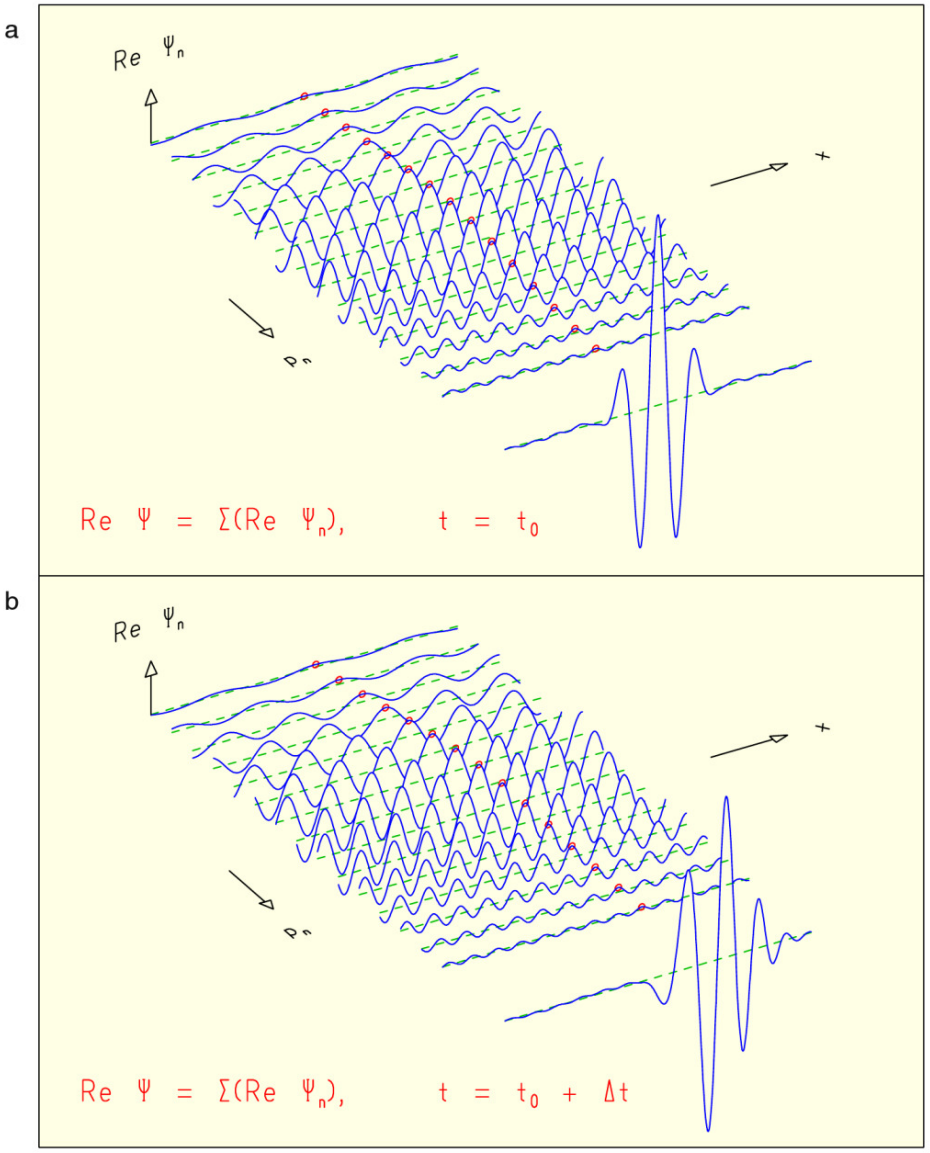

Fig. 3.1. Construction of a wave packet as a sum of harmonic waves ψ_n of different momenta and consequently of different wavelengths. Plotted are the real parts of the wave functions. The terms of different momenta and different amplitudes begin with the one of longest wavelength in the background. In the foreground is the wave packet resulting from the summation. (a) The situation for time $t = t_0$. All partial waves are marked by a circle at point $x = x_0$. (b) The same wave packet and its partial waves at time $t_1 > t_0$. The partial waves have moved different distances $\Delta x_n = v_n(t_1 - t_0)$ because of their different phase velocities v_n, as indicated by the circular marks which have kept their phase with respect to those in part a. Because of the different phase velocities, the wave packet has changed its form and width.

$$M(x,t) = \frac{1}{(2\pi)^{1/4}\sqrt{\sigma_x}} \exp\left[-\frac{(x - x_0 - v_0 t)^2}{4\sigma_x^2}\right]$$

travels in x direction with the *group velocity*

$$v_0 = \frac{p_0}{m} \quad .$$

The group velocity is indeed the particle velocity and different from the phase velocity. The localization in space is given by

$$\sigma_x^2 = \frac{\hbar^2}{4\sigma_p^2}\left(1 + \frac{4\sigma_p^4}{\hbar^2}\frac{t^2}{m^2}\right) \quad .$$

This formula shows that the spatial extension σ_x of the wave packet increases with time. This phenomenon is called *dispersion*. Figure 3.2 shows the time developments of the real and imaginary parts of two wave packets with different group velocities and widths. We easily observe the dispersion of the wave packets in time. The fact that a wave packet comprises a whole range of momenta is the physical reason why it disperses. Its components move with different velocities, thus spreading the packet in space.

The function $\phi(x,t)$ determines the phase of the carrier wave. It has the form

$$\phi(x,t) = \frac{1}{\hbar}\left[p_0 + \frac{\sigma_p^2}{\sigma_x^2}\frac{v_0 t}{2p_0}(x - x_0 - v_0 t)\right](x - x_0 - v_0 t) + \frac{p_0}{2\hbar}v_0 t - \frac{\alpha}{2}$$

with

$$\tan\alpha = \frac{2}{\hbar}\frac{\sigma_p^2}{m}\, t \quad .$$

For fixed time t it represents the phase of a harmonic wave modulated in wave number. The effective wave number k_{eff} is the factor in front of $x - x_0 - v_0 t$ and is given by

$$k_{\text{eff}}(x) = \frac{1}{\hbar}\left[p_0 + \frac{\sigma_p^2}{\sigma_x^2}\frac{v_0 t}{2p_0}(x - x_0 - v_0 t)\right] \quad .$$

At the value $x = \langle x \rangle$ corresponding to the maximum value of the bell-shaped amplitude modulation $M(x,t)$, that is, its position average

$$\langle x \rangle = x_0 + v_0 t \quad ,$$

the effective wave number is simply equal to the wave number that corresponds to the average momentum p_0 of the spectral function,

$$k_0 = \frac{1}{\hbar}p_0 = \frac{1}{\hbar}m v_0 \quad .$$

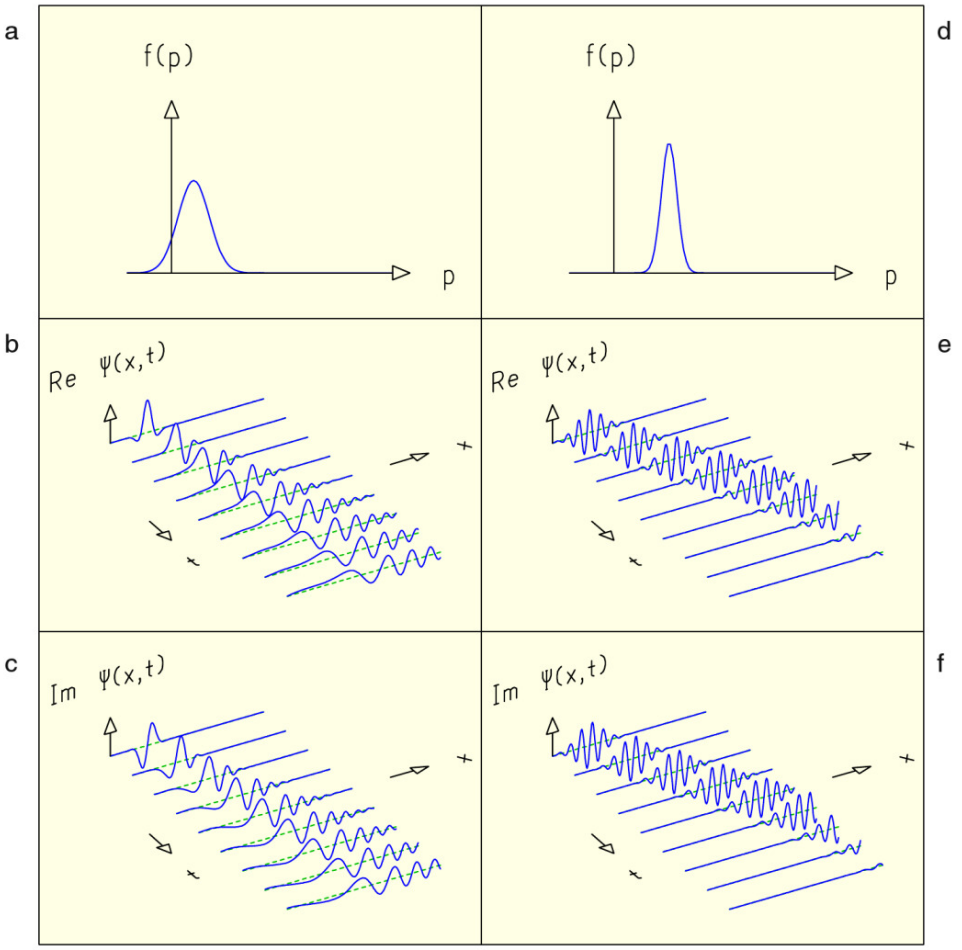

Fig. 3.2. (a, d) Spectral functions and time developments of (b, e) the real parts and (c, f) the imaginary parts of the wave functions for two different wave packets. The two packets have different group velocities and different widths and spread differently with time.

For values $x > x_0 + v_0 t$, that is, in front of the average position $\langle x \rangle$ of the moving wave packet, the effective wave number increases,

$$k_{\text{eff}}(x > x_0 + v_0 t) > k_0 \quad ,$$

so that the local wavelength

$$\lambda_{\text{eff}}(x) = \frac{2\pi}{|k_{\text{eff}}(x)|}$$

decreases.

For values $x < x_0 + v_0 t$, that is, behind the average position $\langle x \rangle$, the effective wave number decreases,

$$k_{\text{eff}}(x < x_0 + v_0 t) < k_0 \quad .$$

This decrease leads to negative values of k_{eff} of large absolute value, which, far behind the average position, makes the wavelengths $\lambda_{\text{eff}}(x)$ short again. This wave number modulation can easily be verified in Figures 3.1 and 3.2. For a wave packet at rest, that is, $p_0 = 0$, $v_0 = p_0/m = 0$, the effective wave number

$$k_{\text{eff}}(x) = \frac{1}{\hbar} \frac{\sigma_p^2}{\sigma_x^2} \frac{t}{2m} (x - x_0)$$

has the same absolute value to the left and to the right of the average position x_0. This implies a decrease of the effective wavelength that is symmetric on both sides of x_0. Figure 3.4 corroborates this statement.

3.3 Probability Interpretation, Uncertainty Principle

Following Max Born (1926), we interpret the wave function $\psi(x,t)$ as follows. Its absolute square

$$\rho(x,t) = |\psi(x,t)|^2 = M^2(x,t)$$

is identified with the *probability density* for observing the particle at position x and time t, that is, the probability of observing the particle at a given time t in the space region between x and $x + \Delta x$ is $\Delta P = \rho(x,t)\,\Delta x$. This is plausible since $\rho(x,t)$ is positive everywhere. Furthermore, its integral over all space is equal to one for every moment in time so that the *normalization condition*

$$\int_{-\infty}^{+\infty} |\psi(x,t)|^2 \,\mathrm{d}x = \int_{-\infty}^{+\infty} \psi^*(x,t)\psi(x,t)\,\mathrm{d}x = 1$$

holds.

Notice, that there is a strong formal similarity between the average energy density $w(x,t) = \varepsilon_0 |E_c(x,t)|^2/2$ of a light wave and the probability density $\rho(x,t)$. Because of the probability character, the wave function $\psi(x,t)$ is not a field strength, since the effect of a field strength must be measurable wherever the field is not zero. A probability density, however, determines the probability that a particle, which can be point-like, will be observed at a given position. This probability interpretation is, however, restricted to normalized wave functions. Since the integral over the absolute square of a harmonic plane wave is

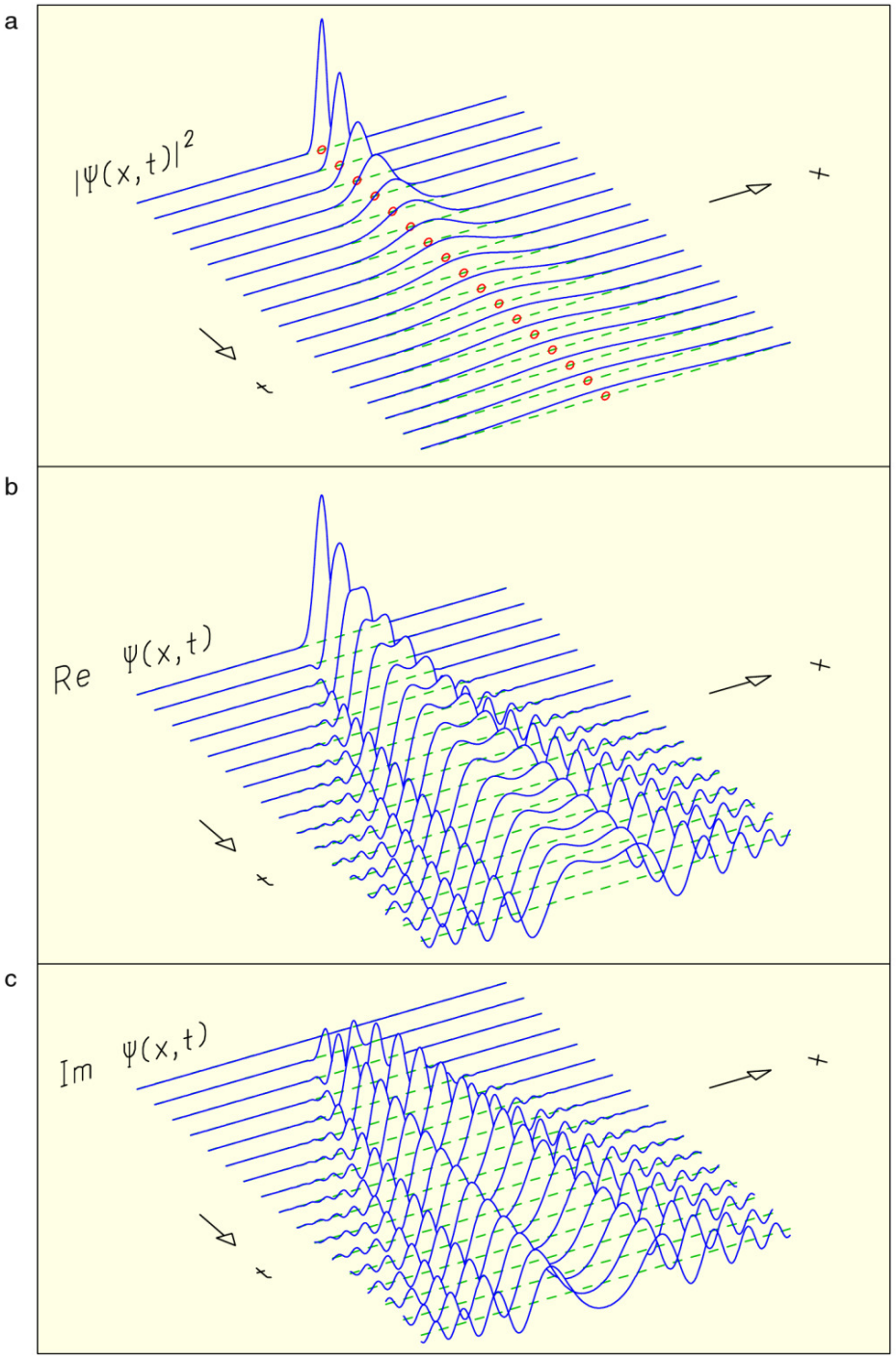

Fig. 3.4. Time developments of the probability density for a wave packet at rest and of the real part and the imaginary part of its wave function.

which, in general, remains a function of time. For a Gaussian wave packet the integration indeed yields

$$\langle x \rangle = x_0 + v_0 t \quad , \qquad v_0 = \frac{p_0}{m} \quad ,$$

corresponding to the trajectory of classical unaccelerated motion. We shall therefore interpret the Gaussian wave packet of de Broglie waves as a quantum-mechanical description of the unaccelerated *motion of a particle*, that is, a particle moving with constant velocity. Actually, the Gaussian form of the spectral function $f(k)$ allows the explicit calculation of the wave packet. With this particular spectral function, the wave function $\psi(x,t)$ can be given in closed form.

The *variance of the position* is the expectation value of the square of the difference between the position and its expectation:

$$\begin{aligned} \mathrm{var}(x) &= \left\langle (x - \langle x \rangle)^2 \right\rangle \\ &= \int_{-\infty}^{+\infty} \psi^*(x,t)(x - \langle x \rangle)^2 \psi(x,t) \mathrm{d}x \quad . \end{aligned}$$

Again, for the Gaussian wave packet the integral can be carried out to give

$$\mathrm{var}(x) = \sigma_x^2 = \frac{\hbar^2}{4\sigma_p^2} \left(1 + \frac{4\sigma_p^4}{\hbar^2} \frac{t^2}{m^2} \right) \quad ,$$

which agrees with the formula quoted in Section 3.2.

Calculation of the expectation value of the momentum of a wave packet

$$\psi(x,t) = \int_{-\infty}^{+\infty} f(p) \psi_p(x - x_0, t) \mathrm{d}p$$

is carried out with the direct help of the spectral function $f(p)$, that is,

$$\langle p \rangle = \int_{-\infty}^{+\infty} p |f(p)|^2 \mathrm{d}p \quad .$$

For the spectral function $f(p)$ of the Gaussian wave packet given at the beginning of Section 3.2, we find

$$\langle p \rangle = \int_{-\infty}^{+\infty} p \frac{1}{\sqrt{2\pi}\sigma_p} \exp\left[-\frac{(p - p_0)^2}{2\sigma_p^2} \right] \mathrm{d}p \quad .$$

We replace the factor p by the identity

$$p = p_0 + (p - p_0) \quad .$$

Since the exponential in the integral above is an even function in the variable $p - p_0$, the integral

$$\int_{-\infty}^{+\infty} (p - p_0) \frac{1}{\sqrt{2\pi}\sigma_p} \exp\left[-\frac{(p-p_0)^2}{2\sigma_p^2} \right] \mathrm{d}p = 0$$

vanishes, for the contributions in the intervals $-\infty < p < p_0$ and $p_0 < p < \infty$ cancel. The remaining term is the product of the constant p_0 and the normalization integral,

$$\int_{-\infty}^{+\infty} |f(p)|^2 \mathrm{d}p = 1 \quad ,$$

so that we find

$$\langle p \rangle = p_0 \quad .$$

This result is not surprising, for the Gaussian spectral function gives the largest weight to momentum p_0 and decreases symmetrically to the left and right of this value. At the end of Section 3.2, we found $v_0 = p_0/m$ as the group velocity of the wave packet. Putting the two findings together, we have discovered that the momentum expectation value of a free, unaccelerated Gaussian wave packet is the same as the momentum of a free, unaccelerated particle of mass m and velocity v_0 in classical mechanics:

$$\langle p \rangle = p_0 = m v_0 \quad .$$

The expectation value of momentum can also be calculated directly from the wave function $\psi(x,t)$. We have the simple relation

$$\begin{aligned} \frac{\hbar}{\mathrm{i}} \frac{\partial}{\partial x} \psi_p(x - x_0, t) &= \frac{\hbar}{\mathrm{i}} \frac{\partial}{\partial x} \left\{ \frac{1}{(2\pi\hbar)^{1/2}} \exp\left[-\frac{\mathrm{i}}{\hbar}(Et - px) \right] \right\} \\ &= p \psi_p(x - x_0, t) \quad . \end{aligned}$$

This relation translates the momentum variable p into the *momentum operator*

$$p \to \frac{\hbar}{\mathrm{i}} \frac{\partial}{\partial x} \quad .$$

The momentum operator allows us to calculate the expectation value of momentum from the following formula:

$$\langle p \rangle = \int_{-\infty}^{+\infty} \psi^*(x,t) \frac{\hbar}{\mathrm{i}} \frac{\partial}{\partial x} \psi(x,t) \mathrm{d}x \quad .$$

It is completely analogous to the formula for the expectation value of position given earlier. We point out that the operator appears between the functions $\psi^*(x,t)$ and $\psi(x,t)$, thus acting on the second factor only. To verify this formula, we replace the wave function $\psi(x,t)$ by its representation in terms of the spectral function:

$$\begin{aligned}\langle p\rangle &= \int_{-\infty}^{+\infty}\psi^*(x,t)\frac{\hbar}{\mathrm{i}}\frac{\partial}{\partial x}\int_{-\infty}^{+\infty}f(p)\psi_p(x-x_0,t)\,\mathrm{d}p\,\mathrm{d}x \\ &= \int_{-\infty}^{+\infty}\int_{-\infty}^{+\infty}\psi^*(x,t)\psi_p(x-x_0,t)\,\mathrm{d}x\;pf(p)\,\mathrm{d}p \quad .\end{aligned}$$

The inner integral

$$\begin{aligned}&\int_{-\infty}^{+\infty}\psi^*(x,t)\psi_p(x-x_0,t)\,\mathrm{d}x \\ &\quad = \int_{-\infty}^{+\infty}\psi^*(x,t)\frac{1}{(2\pi\hbar)^{1/2}}\exp\left\{-\frac{\mathrm{i}}{\hbar}\left[Et-p(x-x_0)\right]\right\}\mathrm{d}x\end{aligned}$$

is by Fourier's theorem the inverse of the representation

$$\begin{aligned}\psi^*(x,t) &= \int_{-\infty}^{+\infty}f^*(p)\psi_p^*(x-x_0,t)\,\mathrm{d}p \\ &= \frac{1}{(2\pi\hbar)^{1/2}}\int_{-\infty}^{+\infty}f^*(p)\exp\left\{\frac{\mathrm{i}}{\hbar}\left[Et-p(x-x_0)\right]\right\}\mathrm{d}p\end{aligned}$$

of the complex conjugate of the wave packet $\psi(x,t)$. Thus we have

$$\int_{-\infty}^{+\infty}\psi^*(x,t)\psi_p(x-x_0,t)\,\mathrm{d}x = f^*(p) \quad .$$

Substituting this result for the inner integral of the expression for $\langle p\rangle$, we rediscover the expectation value of momentum in the form

$$\langle p\rangle = \int_{-\infty}^{+\infty}f^*(p)pf(p)\,\mathrm{d}p = \int_{-\infty}^{+\infty}p|f(p)|^2\,\mathrm{d}p \quad .$$

This equation justifies the identification of momentum p with the operator $(\hbar/\mathrm{i})(\partial/\partial x)$ acting on the wave function. The *variance of the momentum* for a wave packet is

$$\mathrm{var}(p) = \langle(p-\langle p\rangle)^2\rangle = \int_{-\infty}^{+\infty}\psi^*(x,t)\left(\frac{\hbar}{\mathrm{i}}\frac{\partial}{\partial x}-p_0\right)^2\psi(x,t)\,\mathrm{d}x \quad .$$

For our Gaussian packet we have

$$\mathrm{var}(p) = \sigma_p^2$$

again independent of time because momentum is conserved.

The square root of the variance of the position,

$$\Delta x = \sqrt{\mathrm{var}(x)} = \sigma_x \quad ,$$

determines the width of the wave packet in the position variable x and therefore is a measure of the *uncertainty* about where the particle is located. By the same token, the corresponding uncertainty about the momentum of the particle is

$$\Delta p = \sqrt{\mathrm{var}(p)} = \sigma_p \quad .$$

For our Gaussian wave packet we found the relation

$$\sigma_x = \frac{\hbar}{2\sigma_p}\left(1+\frac{4\sigma_p^4}{\hbar^2}\frac{t^2}{m^2}\right)^{1/2} \quad .$$

For time $t = 0$ this relation reads

$$\sigma_x \sigma_p = \frac{\hbar}{2} \quad .$$

For later moments in time, the product becomes even larger so that, in general,

$$\Delta x \cdot \Delta p \geq \frac{\hbar}{2} \quad .$$

This relation expresses the fact that the product of uncertainties in position and momentum cannot be smaller than the fundamental Planck's constant h divided by 4π.

We have just stated the *uncertainty principle*, which is valid for wave packets of all forms. It was formulated by Werner Heisenberg in 1927. This relation says, in effect, that a small uncertainty in localization can only be achieved at the expense of a large uncertainty in momentum and vice versa. Figure 3.5 illustrates this principle by comparing the time development of the probability density $\rho(x,t)$ and the square of the spectral function $f^2(p)$. The latter, in fact, is the probability density in momentum. Looking at the spreading of the wave packets with time, we see that the initially narrow wave packet (Figure 3.5, top right) becomes quickly wide in space, whereas the initially wide wave packet (Figure 3.5, bottom right) spreads much more slowly. Actually, this behavior is to be expected. The spatially narrow wave packet requires a wide spectral function in momentum space. Thus it comprises components with a wide range of velocities. They, in turn, cause a quick dispersion of the packet in space compared to the initially wider packet with a narrower spectral function (Figures 3.5, bottom left and bottom right).

At its initial time $t = 0$ the Gaussian wave packet discussed at the beginning of Section 3.2 has the smallest spread in space and momentum because Heisenberg's uncertainty principle is fulfilled in the equality form $\sigma_x \cdot \sigma_p = \hbar/2$. The wave function at $t = 0$ takes the simple form

$$\begin{aligned}\psi(x,0) &= \frac{1}{(2\pi)^{1/4}\sqrt{\sigma_x}}\exp\left[-\frac{(x-x_0)^2}{4\sigma_x^2}\right]\exp\left[\frac{\mathrm{i}}{\hbar}p_0(x-x_0)\right] \\ &= M(x,0)\exp[\mathrm{i}\phi(x,0)] \quad .\end{aligned}$$

The bell-shaped amplitude function $M(x,0)$ is centered around the position x_0 with the width σ_x; ϕ is the phase of the wave function at $t = 0$ and has the simple linear dependence

$$i\hbar \frac{\partial}{\partial t}\psi(x,t) = -\frac{\hbar^2}{2m}\frac{\partial^2}{\partial x^2}\psi(x,t) + V(x)\psi(x,t) \quad .$$

We now denote the operator of total energy by the symbol

$$H = -\frac{\hbar^2}{2m}\frac{\partial}{\partial x} + V(x) \quad .$$

In analogy to the Hamilton function of classical mechanics, operator H is called the *Hamilton operator* or *Hamiltonian*. With its help the Schrödinger equation for the motion of a particle under the influence of a potential takes the form

$$i\hbar \frac{\partial}{\partial t}\psi(x,t) = H\psi(x,t) \quad .$$

At this stage we should point out that the Schrödinger equation, generalized to three spatial dimensions and many particles, is the fundamental law of nature for all of nonrelativistic particle physics and chemistry. The rest of this book will be dedicated to the pictorial study of the simple phenomena described by the Schrödinger equation.

3.5 Bivariate Gaussian Probability Density

To facilitate the physics discussion in the next section we now introduce a *Gaussian probability density of two variables* x_1 and x_2 and demonstrate its properties. The bivariate Gaussian probability density is defined by

$$\begin{aligned}\rho(x_1,x_2) \;=\; & A\exp\left\{-\frac{1}{2(1-c^2)}\left[\frac{(x_1-\langle x_1\rangle)^2}{\sigma_1^2}\right.\right. \\ & \left.\left. -\,2c\frac{(x_1-\langle x_1\rangle)}{\sigma_1}\frac{(x_2-\langle x_2\rangle)}{\sigma_2} + \frac{(x_2-\langle x_2\rangle)^2}{\sigma_2^2}\right]\right\} \quad .\end{aligned}$$

The normalization constant

$$A = \frac{1}{2\pi\sigma_1\sigma_2\sqrt{1-c^2}}$$

ensures that the probability density is properly normalized:

$$\int_{-\infty}^{+\infty}\int_{-\infty}^{+\infty}\rho(x_1,x_2)\,dx_1\,dx_2 = 1 \quad .$$

The bivariate Gaussian is completely described by five parameters. They are the *expectation values* $\langle x_1\rangle$ and $\langle x_2\rangle$, the *widths* σ_1 and σ_2, and the *correlation coefficient* c. The *marginal distributions* defined by

$$\rho_1(x_1) = \int_{-\infty}^{+\infty} \rho(x_1,x_2)\mathrm{d}x_2 \quad ,$$
$$\rho_2(x_2) = \int_{-\infty}^{+\infty} \rho(x_1,x_2)\mathrm{d}x_1$$

are for the bivariate Gaussian distribution simply Gaussians of a single variable,

$$\rho_1(x_1) = \frac{1}{\sqrt{2\pi}\sigma_1}\exp\left[-\frac{(x_1-\langle x_1\rangle)^2}{2\sigma_1^2}\right] \quad ,$$
$$\rho_2(x_2) = \frac{1}{\sqrt{2\pi}\sigma_2}\exp\left[-\frac{(x_2-\langle x_2\rangle)^2}{2\sigma_2^2}\right] \quad .$$

Each marginal distribution depends on two parameters only, the expectation value and the width of its variable.

Lines of constant probability density in x_1, x_2 are the lines of intersection between the surface $\rho(x_1,x_2)$ and a plane $\rho = a = \text{const}$.

One particular ellipse, for which

$$\rho(x_1,x_2) = A\exp\left\{-\frac{1}{2}\right\} \quad ,$$

i.e., the one for which the exponent in the bivariate Gaussian is simply equal to $-1/2$, is called the *covariance ellipse*. Points x_1, x_2 on the covariance ellipse fulfill the equation

$$\frac{1}{1-c^2}\left\{\frac{(x_1-\langle x_1\rangle)^2}{\sigma_1^2} - 2c\frac{(x_1-\langle x_1\rangle)}{\sigma_1}\frac{(x_2-\langle x_2\rangle)}{\sigma_2} + \frac{(x_2-\langle x_2\rangle)^2}{\sigma_2^2}\right\} = 1 \quad .$$

Projected on the x_1 axis and the x_2 axis, it yields lines of lengths $2\sigma_1$ and $2\sigma_2$, respectively.

The plots in Figure 3.6 differ only by the value c of the covariance. The covariance ellipses are shown as lines of constant probability on the surfaces $\rho(x_1,x_2)$. For $c = 0$ the principal axes of the covariance ellipse are parallel to the coordinate axes. In this situation variables x_1 and x_2 are *uncorrelated*, that is, knowledge that $x_1 > \langle x_1\rangle$ holds true does not tell us whether it is more probable to observe $x_2 > \langle x_2\rangle$ or $x_2 < \langle x_2\rangle$. For uncorrelated variables the relation between the joint probability density and the marginal distribution is simple, $\rho(x_1,x_2) = \rho_1(x_1)\rho_2(x_2)$. The situation is different for correlated variables, that is, for $c \neq 0$. For a positive correlation, $c > 0$, the major axis of the ellipse lies along a direction between those of the x_1 axis and the x_2 axis. If we know that $x_1 > \langle x_1\rangle$ is valid it is more probable to have $x_2 > \langle x_2\rangle$ than to have $x_2 < \langle x_2\rangle$. If, on the other hand, the correlation is negative, $x < 0$, the major axis has a direction between those of the x_1 axis and the negative

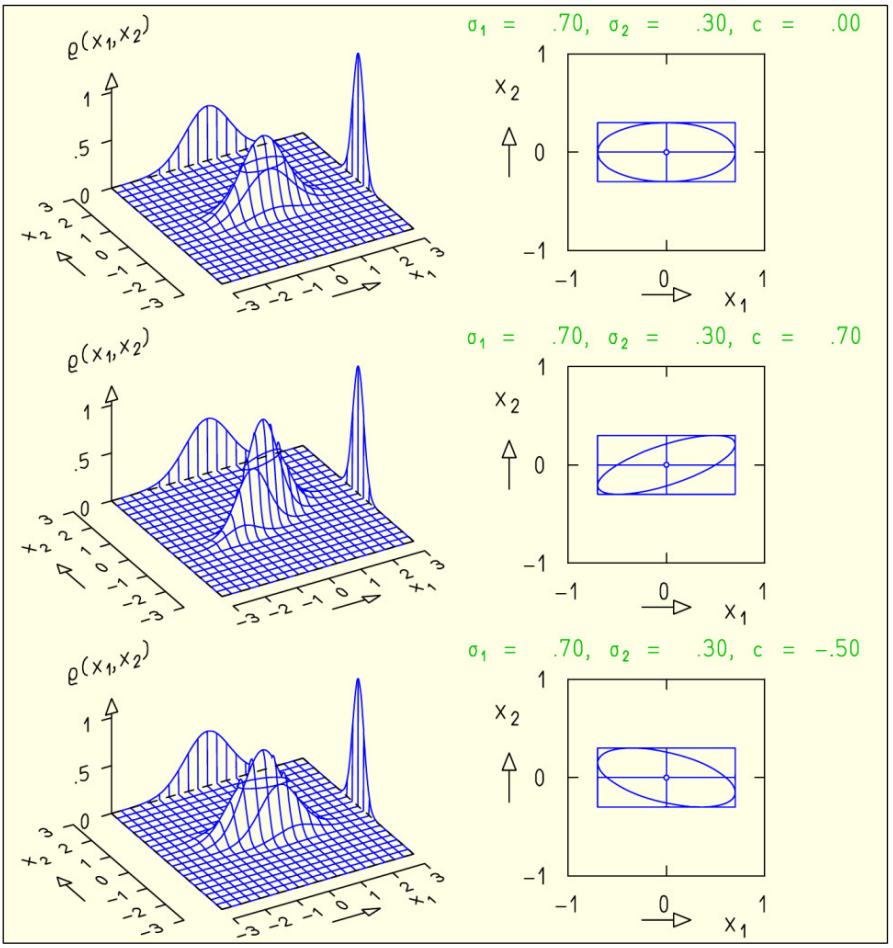

Fig. 3.6. Bivariate Gaussian probability density $\rho(x_1,x_2)$ drawn as a surface over the x_1,x_2 plane and marginal distributions $\rho_1(x_1)$ and $\rho_2(x_2)$. The latter are drawn as curves over the margins parallel to the x_1 axis and the x_2 axis, respectively. Also shown is the covariance ellipse corresponding to the distribution. The rectangle circumscribing the ellipse has the sides $2\sigma_1$ and $2\sigma_2$, respectively. The pairs of plots in the three rows of the figure differ only by the correlation coefficient c.

x_2 axis. In this situation, once it is known that $x_1 > \langle x_1 \rangle$ is valid, $x_2 < \langle x_2 \rangle$ is more probable than $x_2 > \langle x_2 \rangle$.

The amount of correlation is measured by the numerical value of c, which can vary in the range $-1 < c < 1$. In the limiting case of total correlation, $c = \pm 1$, the covariance ellipse degenerates to a line, the principal axis. The joint probability density is completely concentrated along this line. That is, knowing the value x_1 of one variable, we also know the value x_2 of the other.

Also shown in Figure 3.6 are the covariance ellipses directly drawn in the x_1, x_2 plane and the rectangles with sides parallel to the x_1 and the x_2 axes. The lengths of these sides are $2\sigma_1$ and $2\sigma_2$, respectively. If there is no correlation ($c = 0$) the principal axes of the ellipse are parallel to the coordinate axes so that the principal semi-axes have lengths σ_1 and σ_2. For $c \neq 0$ the principal axes form an angle α with the coordinate axes. The angle α is given by

$$\tan 2\alpha = \frac{2c\sigma_1\sigma_2}{\sigma_1^2 - \sigma_2^2} \quad .$$

3.6 Comparison with a Classical Statistical Description

The interpretation of the wave-packet solution as a classical point particle catches only the most prominent and simplest classical features of particle motion. To exploit our intuition of classical mechanics somewhat further, we study a classical point particle with initial position and momentum known to some inaccuracy only. In principle, such a situation prevails in all classical mechanical systems because of the remaining inaccuracy of the initial conditions due to errors inevitable even in all classical measurements. The difference in principle compared to quantum physics is, however, that according to the laws of classical physics the errors in location and momentum of a particle both can be made arbitrarily small independent of each other. From Heisenberg's uncertainty principle we know that this is not possible in quantum physics.

We now study the motion of a classical particle described at the initial time $t = 0$ by a joint probability density in location and momentum which we choose to be a bivariate Gaussian about the average values x_0 and p_0 with the widths σ_{x0} and σ_p. We assume that at the initial time $t = 0$ there is no correlation between position and momentum. The initial joint probability density is then

$$\rho_{\mathrm{i}}^{\mathrm{cl}}(x,p) = \frac{1}{\sqrt{2\pi}\sigma_{x0}} \exp\left\{-\frac{(x-x_0)^2}{2\sigma_{x0}^2}\right\} \frac{1}{\sqrt{2\pi}\sigma_p} \exp\left\{-\frac{(p-p_0)^2}{2\sigma_p^2}\right\} \quad .$$

For force-free motion the particle does not suffer a change in momentum as time elapses, e.g., also at a later time $t > 0$ the particle still moves with its initial momentum, i.e., $p = p_{\mathrm{i}}$. Thus, the momentum distribution does not change with time. The position of a particle of momentum p_{i} at time t initially having the position x_{i} is given by

$$x = x_{\mathrm{i}} + v_{\mathrm{i}} t \quad , \qquad v_{\mathrm{i}} = p_{\mathrm{i}}/m \quad .$$

The probability density initially described by $\rho_{\mathrm{i}}^{\mathrm{cl}}(x_{\mathrm{i}}, p_{\mathrm{i}})$ can be expressed at time t by the positions x at time t by inserting

$$x_{\rm i} = x - (p/m)t \quad ,$$

yielding the *classical phase-space probability density*

$$\begin{aligned}\rho^{\rm cl}(x,p,t) &= \rho_{\rm i}^{\rm cl}(x - pt/m, p) \\ &= \frac{1}{2\pi\sigma_{x0}\sigma_p}\exp\left\{-\frac{1}{2}\left[\frac{(x - x_0 - pt/m)^2}{\sigma_{x0}^2} + \frac{(p-p_0)^2}{\sigma_p^2}\right]\right\} \\ &= \frac{1}{2\pi\sigma_{x0}\sigma_p}\exp L \quad .\end{aligned}$$

The exponent is a quadratic polynomial in x and p which can be written as

$$\begin{aligned}L &= -\frac{1}{2}\left\{\frac{(x - [x_0 + p_0 t/m] - (p-p_0)t/m)^2}{\sigma_{x0}^2} + \frac{(p-p_0)^2}{\sigma_p^2}\right\} \\ &= -\frac{1}{2}\frac{\sigma_{x0}^2 + \sigma_p^2 t^2/m^2}{\sigma_{x0}^2}\left\{\frac{(x - [x_0 + p_0 t/m])^2}{\sigma_{x0}^2 + \sigma_p^2 t^2/m^2}\right. \\ &\quad \left. - \frac{2(x - [x_0 + p_0 t/m])(p-p_0)}{(\sigma_{x0}^2 + \sigma_p^2 t^2/m^2)m/t} + \frac{(p-p_0)^2}{\sigma_p^2}\right\} \quad .\end{aligned}$$

Comparing this expression with the exponent of the general expression for a bivariate probability density in Section 3.5 we find that $\rho^{\rm cl}(x,p,t)$ is a bivariate Gaussian with the expectation values

$$\langle x(t)\rangle = x_0 + p_0 t/m \quad , \qquad \langle p(t)\rangle = p_0 \quad ,$$

the widths

$$\sigma_x(t) = \sqrt{\sigma_{x0}^2 + \sigma_p^2 t^2/m^2} \quad , \qquad \sigma_p(t) = \sigma_p \quad ,$$

and the correlation coefficient

$$c = \frac{\sigma_p t}{\sigma_x(t) m} = \frac{\sigma_p t/m}{\sqrt{\sigma_{x0}^2 + \sigma_p^2 t^2/m^2}} \quad .$$

In particular this means that the marginal distribution $\rho_x^{\rm cl}(x,t)$, i.e., the spatial probability density for the classical particle with initial uncertainties σ_{x0} in position and σ_p momentum is

$$\rho_x^{\rm cl}(x,t) = \frac{1}{\sqrt{2\pi}\sigma_x(t)}\exp\left\{-\frac{(x - [x_0 + p_0 t/m])^2}{2\sigma_x^2(t)}\right\} \quad .$$

Let us now study the classical probability density $\rho^{\rm cl}(x,p,t)$ of a particle with initial uncertainties σ_{x0} in position and σ_p in momentum which satisfy the minimal uncertainty requirement of quantum mechanics:

$$\sigma_{x0}\sigma_p = \hbar/2 \quad .$$

Problems

3.1. Calculate the de Broglie wavelengths and frequencies of an electron and a proton that have been accelerated by an electric field through a potential difference of 100 V. What are the corresponding group and phase velocities?

3.2. An electron represented by a Gaussian wave packet with average energy $E_0 = 100\,\text{eV}$ was initially prepared to have momentum width $\sigma_p = 0.1\,p_0$ and position width $\sigma_x = \hbar/(2\sigma_p)$. How much time elapses before the wave packet has spread to twice the original spatial extension?

3.3. Show that the normalization condition $\int_{-\infty}^{+\infty} |\psi(x,t)|^2\,\mathrm{d}x = 1$ holds true for any time if $\psi(x,t)$ is a Gaussian wave packet with a normalized spectral function $f(p)$.

3.4. Calculate the action of the commutator $[p,x] = px - xp$, $p = (\hbar/\mathrm{i})(\partial/\partial x)$ on a wave function $\psi(x,t)$. Show that it is equivalent to the multiplication of $\psi(x,t)$ by $\hbar/\mathrm{i}$ so that we may write $[p,x] = \hbar/\mathrm{i}$.

3.5. Express the expectation value of the kinetic energy of a Gaussian wave packet in terms of the expectation value of the momentum and the width σ_p of the spectral function.

3.6. Given a Gaussian wave packet of energy expectation value $\langle E\rangle$ and momentum expectation value $\langle p\rangle$, write its normalized spectral function $f(p)$.

3.7. A large virus may for purposes of this problem be approximated by a cube whose sides measure one micron and which has the density of water. Assuming as an upper estimate an uncertainty of one micron in position, calculate the minimum uncertainty in velocity of the virus.

3.8. The radius of both the proton and the neutron is measured to be of the order of $10^{-15}\,\text{m}$. A free neutron decays spontaneously into a proton, an electron, and a neutrino. The momentum of the emitted electron is typically $1\,\text{MeV}/c$. If the neutron were, as once thought, a bound system consisting of a proton and an electron, how large would be the position uncertainty of the electron and hence the size of the neutron? Take as the momentum uncertainty of the electron the value $1\,\text{MeV}/c$.

3.9. Show that the solutions of the Schrödinger equation satisfy the continuity equation

$$\frac{\partial \rho(x,t)}{\partial t} + \frac{\partial j(x,t)}{\partial x} = 0$$

for the probability density

$$\rho(x,t) = \psi^*(x,t)\psi(x,t)$$

and the probability current density

$$j(x,t) = \frac{\hbar}{2\mathrm{i}m}\left[\psi^*(x,t)\frac{\partial}{\partial x}\psi(x,t) - \psi(x,t)\frac{\partial}{\partial x}\psi^*(x,t)\right] \quad .$$

To this end, multiply the Schrödinger equation by $\psi^*(x,t)$ and its complex conjugate

$$\mathrm{i}\hbar\frac{\partial \psi^*(x,t)}{\partial t} = \frac{\hbar^2}{2m}\frac{\partial^2}{\partial x^2}\psi^*(x,t) - V(x)\psi^*(x,t)$$

by $\psi(x,t)$, and add the two resulting equations.

3.10. Convince yourself with the help of the continuity equation that the normalization integral

$$\int_{-\infty}^{+\infty} \psi^*(x,t)\psi(x,t)\,\mathrm{d}x$$

is independent of time if $\psi(x,t)$ is a normalized solution of the Schrödinger equation. To this end, integrate the continuity equation over all x and use the vanishing of the wave function for large $|x|$ to show the vanishing of the integral over the probability current density.

3.11. Calculate the probability current density for the free Gaussian wave packet as given at the end of Section 3.2. Interpret the result for $t = 0$ in terms of the probability density and the group velocity of the packet.

3.12. Show that the one-dimensional Schrödinger equation possesses spatial reflection symmetry, that is, is invariant under the substitution $x \to -x$ if the potential is an even function, that is, $V(x) = V(-x)$.

3.13. Show that the *ansatz* for the Gaussian wave packet of Section 3.2 fulfills the Schrödinger equation for a free particle.

4. Solution of the Schrödinger Equation in One Dimension

4.1 Separation of Time and Space Coordinates, Stationary Solutions

The simple structure of the Schrödinger equation allows a particular *ansatz* in which the time and space dependences occur in separate factors,

$$\psi_E(x,t) = \exp\left(-\frac{\mathrm{i}}{\hbar}Et\right)\varphi_E(x) \quad .$$

As in the case of electromagnetic waves, we call the factor $\varphi_E(x)$ that is independent of time a *stationary solution*. Inserting our *ansatz* into the Schrödinger equation yields an equation for the stationary wave,

$$-\frac{\hbar^2}{2m}\frac{\mathrm{d}^2}{\mathrm{d}x^2}\varphi_E(x) + V(x)\varphi_E(x) = E\varphi_E(x) \quad ,$$

which is often called the *time-independent Schrödinger equation*. It is characterized by the parameter E, which is called an *eigenvalue*. The left-hand side represents the sum of the kinetic and the potential energy, so that E is the total energy of the stationary solution. The solution $\varphi_E(x)$ is called an *eigenfunction* of the Hamilton operator

$$H = -\frac{\hbar^2}{2m}\frac{\mathrm{d}^2}{\mathrm{d}x^2} + V(x) \quad ,$$

since the time-independent Schrödinger equation can be put into the form

$$H\varphi_E(x) = E\varphi_E(x) \quad .$$

We also say that the solution $\varphi_E(x)$ describes an *eigenstate* of the system specified by the Hamilton operator. This eigenstate is characterized by the eigenvalue E of the total energy. Often the stationary solution $\varphi_E(x)$ is also called a *stationary state* of the system.

S. Brandt and H.D. Dahmen, *The Picture Book of Quantum Mechanics*,
DOI 10.1007/978-1-4614-3951-6_4, © Springer Science+Business Media New York 2012

The time-independent Schrödinger equation has a large manifold of solutions. It is supplemented by *boundary conditions* that have to be imposed on a particular solution. These boundary conditions must be abstracted from the physical process that the solution should describe. The boundary conditions on the solution for the elastic scattering in one dimension of a particle under the action of a force will be discussed in the next section. Because of the boundary conditions, solutions $\varphi_E(x)$ exist for particular values of the energy eigenvalues or for particular energy intervals only.

As a first example, we look at the de Broglie waves,

$$\psi_p(x-x_0,t) = \frac{1}{(2\pi\hbar)^{1/2}} \exp\left[-\frac{\mathrm{i}}{\hbar}(Et - px + px_0)\right] \quad .$$

The function $\psi_p(x-x_0,t)$ factors into $\exp[-(\mathrm{i}/\hbar)Et]$ and the stationary wave

$$\frac{1}{(2\pi\hbar)^{1/2}} \exp\left[\frac{\mathrm{i}}{\hbar}p(x-x_0)\right] \quad .$$

It is a solution of the time-independent Schrödinger equation with a vanishing potential for the energy eigenvalue $E = p^2/2m$. A superposition of de Broglie waves fulfilling the normalization condition of Section 3.3 forms a wave packet describing an unaccelerated particle. Here x_0 is the position expectation value of the wave packet at time $t = 0$.

Since the momentum p is a real parameter, the energy eigenvalue of a de Broglie wave is always positive. Thus, for the case of de Broglie waves, we have found the restriction $E \geq 0$ for the energy eigenvalues.

The general solution of the time-dependent Schrödinger equation is given by a linear combination of waves of different energies. This is tantamount to stating that the various components of different energy E superimposed in the solution change independently of one another with time.

For initial time $t = 0$ the functions ψ_E and φ_E coincide. An initial condition prescribed at $t = 0$ determines the coefficients in the linear combination of spectral components of different energies. Therefore the procedure for solving the equation for a given initial condition has three steps. First, we determine the stationary solutions $\varphi_E(x)$ of the time-independent Schrödinger equation. Second, we superimpose them with appropriate coefficients to reproduce the initial condition $\psi(x,0)$ at $t = 0$. Finally, we introduce into every term of this linear combination the time-dependent factor $\exp[-(\mathrm{i}/\hbar)Et]$ corresponding to the energy of the stationary solution φ_E and sum them up to give $\psi(x,t)$, the solution of the time-dependent Schrödinger equation.

In the next section we study methods of obtaining the stationary solutions.

4.2 Stationary Scattering Solutions: Piecewise Constant Potential

As in classical mechanics, the scattering of a particle by a force is called elastic if only its momentum is changed while its energy is conserved. A force is said to be of finite range if it is practically zero for distances from the center of force larger than a finite distance d. This distance d is called the range of the force. The elastic scattering of a particle through a force of finite range consists of three stages subsequent in time.

1. The incoming particle moves unaccelerated in a force-free region toward the range of the force.
2. The particle moves under the influence of the force. The action of the force changes the momentum of the particle.
3. After the scattering the outgoing particle moves away from the range of the force. Its motion in the force-free region is again unaccelerated.

In Section 3.3 we have seen that the force-free motion of a particle of mass m can be described by a wave packet of de Broglie waves,

$$\begin{aligned} \psi_p(x-x_0,t) &= \frac{1}{(2\pi\hbar)^{1/2}} \exp\left[-\frac{\mathrm{i}}{\hbar}(Et - px + px_0)\right] \quad , \\ E &= \frac{p^2}{2m} \quad . \end{aligned}$$

They can be factored into the time-dependent factor $\exp[-(\mathrm{i}/\hbar)Et]$ and the stationary wave $(2\pi\hbar)^{-1/2}\exp[(\mathrm{i}/\hbar)p(x-x_0)]$. This stationary wave is a solution of the time-independent Schrödinger equation with a vanishing potential.

If the spectral function $f(p)$ of the wave packet has values different from zero in a range of positive p values, the wave packet

$$\begin{aligned} \psi(x,t) &= \int_{-\infty}^{+\infty} f(p)\psi_p(x-x_0,t)\,\mathrm{d}p \\ &= \int_{-\infty}^{+\infty} f(p)\exp\left(-\frac{\mathrm{i}}{\hbar}Et\right)\frac{1}{(2\pi\hbar)^{1/2}}\exp\left[\frac{\mathrm{i}}{\hbar}p(x-x_0)\right]\mathrm{d}p \end{aligned}$$

moves along the x axis from left to right, that is, in the direction of increasing x values.

Now we superimpose de Broglie waves of momentum $-p$,

$$\begin{aligned} \psi_{-p}(x-x_0,t) &= \frac{1}{(2\pi\hbar)^{1/2}} \exp\left[-\frac{\mathrm{i}}{\hbar}(Et + px - px_0)\right] \quad , \\ E &= \frac{p^2}{2m} \quad , \end{aligned}$$